SOME ASPECTS OF LARGE SCALE NUMERICAL MODELLING OF THE ATMOSPHERE

by

D. M. Burridge

European Centre for Medium
Range Weather Forecasts,
Shinfield Park, Reading,
Berkshire, England.

Seminar 1979

LIST OF CONTENTS PAGE

SOME ASPECTS OF LARGE SCALE NUMERICAL MODELLING OF THE ATMOSPHERE

INTRODUCTION

This short series of lectures is concerned with some fundamental aspects of numerical modelling which have relevance to the problem of medium range weather forecasting. The subject matter is weighted towards the problems that have arisen in the design and development of the European Centre's first operational forecasting models. Where possible the Centre's models and/or algorithms are used to illustrate particular concepts and procedures.

For an up-to-date review of the computational aspects of numerical weather prediction models and climate models, readers are referred to Volume 17 of "Methods in Computational Physics" (1977) edited by Chang et al. The chapter by Arakawa and Lamb is recommended particularly for its in depth analysis of the many problems that face the numerical modeller. The number of numerical techniques employed in forecasting models has, in the last 15 years, grown enormously and the Joint Organising Committee of the GARP's recognition of this led to their decision to publish a review of the numerical methods used in atmosphere models. Volume I of this review, GARP Publications Series No. 17, by Mesinger and Arakawa (1976), discusses time stepping schemes and grid point finite differences for the horizontal derivatives. Volume II, edited by Kasahara, which will appear in the near future, contains, amongst other subjects, comprehensive reviews of spectral methods, global mapping problems and finite element methods.

In my first two lectures I shall discuss some of the physical principles that guided the selection of our first operational model, a global grid point model. The ideas are, of course, quite general and apply equally well to the design of spectral and finite element models. In the

third lecture I shall describe the formulation of the Centre's global semi-implicit grid point model and present objective and subjective comparisons of explicit and semi-implicit forecasts. Finally, the fourth lecture gives an introduction to some of the problems that arise in the design of lateral boundary schemes for limited area models.

1. FINITE DIFFERENCE SCHEMES FOR PRIMITIVE EQUATION BAROTROPIC MODELS

1.1 Distribution of variables over a horizontal grid

It is not obvious a priori how one should proceed with the problem of selecting a horizontal grid and the spatial arrangement of the dependent variables. We were guided by the work and suggestions of Arakawa and his co-workers at U.C.L.A. He considered five arrangements, see figure (1.1), of the three dependent variables, horizontal velocity components u and v and the free surface geopotential ϕ, of a barotropic primitive equation model. He was concerned with two fundamental problems, namely accurate simulation of the geostrophic adjustment process and simulation of quasi-geostrophic non-divergent flow. He ruled out grids (A) and (D) as being inferior in their ability to simulate geostrophic adjustment. The choice between the remaining grids is less clear, the relative performance depending on the radius of deformation and the grid spacing. Arakawa selected the C grid for his low resolution general circulation model. Recently, Mesinger (1979) has considered the relative performance of these five grids for the simulation of slow geostrophic motion. His main conclusion is that the A-grid arrangement gives the poorest accuracy, but he was unable to find any clear advantage for any of the remaining four grids. Early in the development of the Centre's grid point model Gauntlett, Burridge and Arpe (1977) compared the performance of the A and C grids in a full primitive equation model with diabatic forcing and their results underlined the superiority of the C grid

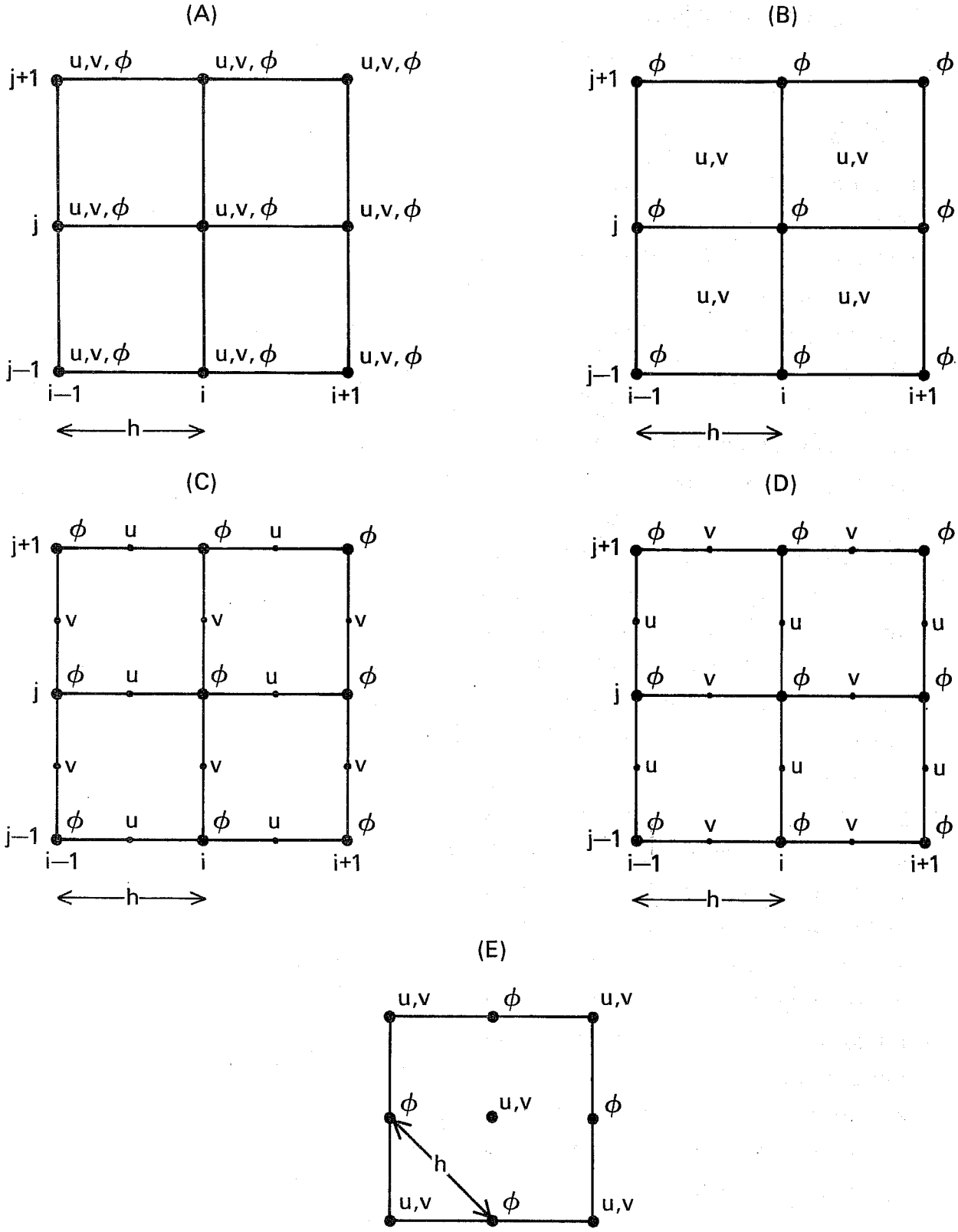

Fig. 1.1 Five grid arrangements for a finite difference description of the barotropic primitive equations. ϕ geopotential; u and v velocity components; h grid length; i and j indices.

over the A grid. We eventually chose the C grid, partly because of its performance with simple models (Arakawa's studies), because of our own experience, but mainly because of its low computational noise and because it lent itself easily to the implementation of a semi-implicit algorithm.

1.2 A global barotropic model

One major problem that has to be considered is the numerical stability of the spatial descretization chosen, whether it is a grid point, finite element or spectral representation. It is now well known that the most potent numerical instabilities arise because the non-linearity of the horizontal advection process can generate, in descrete models, aliasing errors. Mainly through the work of Arakawa (1966) and Lilly (1965), the meteorological community has come to appreciate the role of some of the important integral constraints satisfied by the continuous equations. In the descrete representation, maintenance of conservation laws for mass, energy and potential enstrophy during vorticity advection by a non-divergent horizontal wind field help to inhibit or prevent non-linear instability. In particular, conservation of potential enstrophy, or enstrophy in non-divergent barotropic flows not only prevents non-linear instability, Arakawa (1966) and Sadourny (1975a), but it is an essential feature of the dynamics in two dimensional barotropic flows and controls the exchanges of energy between different scales of motion. Failure to conserve enstrophy accurately in two dimensional flows eventually leads to a spurious computational cascade of energy to small scales, Sadourny (1975a). The use of ad hoc lateral diffusion schemes can control the false numerical cascade by removing energy directly at the small scale end of the spectrum, but a false energy cascade into these scales in combination with excessive lateral smoothing enhances artifically the energy dissipation.

For our first evaluation of various finite difference schemes we used the global barotropic primitive equation model whose governing equations are:

$$\frac{\partial u}{\partial t} - \frac{z}{\cos(\theta)}(\phi v\cos(\theta)) + \frac{1}{a\cos(\theta)}\frac{\partial}{\partial\lambda}(\phi+\tfrac{1}{2}(u^2+v^2)) = 0 \quad (1.1)$$

$$\frac{\partial v}{\partial t} + z\phi u + \frac{1}{a}\frac{\partial}{\partial\theta}(\phi+\tfrac{1}{2}(u^2+v^2)) = 0 \quad (1.2)$$

$$\frac{\partial \phi}{\partial t} + \frac{1}{a\cos(\theta)}\left\{\frac{\partial}{\partial\lambda}(\phi u) + \frac{\partial}{\partial\theta}(\phi v\cos(\theta))\right\} = 0 \quad (1.3)$$

where

$$z = \left\{ f + \frac{1}{a\cos(\theta)}\left(\frac{\partial v}{\partial\lambda} - \frac{\partial}{\partial\theta}(u\cos(\theta))\right)\right\}/\phi \quad (1.4)$$

is the potential vorticity.

This system has the following conservation laws:-

$$\frac{\partial}{\partial t}\int_0^{\pi}\int_0^{2\pi} \phi\cos(\theta)a^2 d\lambda d\theta = 0, \text{ conservation of "mass"}; \quad (1.5)$$

$$\frac{\partial}{\partial t}\int_0^{\pi}\int_0^{2\pi} \frac{1}{a\cos(\theta)}\left\{\frac{\partial v}{\partial\lambda} - \frac{\partial}{\partial\theta}(u\cos(\theta))\right\}\cos(\theta)a^2 d\lambda d\theta = 0, \text{ conservation of vorticity}; \quad (1.6)$$

$$\frac{\partial}{\partial t}\int_0^{\pi}\int_0^{2\pi} \left\{\frac{\phi^2}{2} + \phi\tfrac{1}{2}(u^2+v^2)\right\} a^2\cos(\theta)d\lambda d\theta = 0, \text{ conservation of energy}; \quad (1.7)$$

and

$$\frac{\partial}{\partial t}\int_0^{\pi}\int_0^{2\pi} z^2\phi a^2\cos(\theta)d\lambda d\theta = 0, \text{ conservation of potential enstrophy.} \quad (1.8)$$

Sadourny (1975a) has shown that formal conservation of potential enstrophy is more important than formal conservation of total energy, in that the potential enstrophy conserving models are inherently more stable and maintain more realistic energy spectra.

For our barotropic models we choose to conserve mass, vorticity and potential enstrophy. Our potential enstrophy conserving model is an extension to a regular latitude/longitude grid of the potential enstrophy conserving model described by Sadourny (1975b) for a global cylindrical coordinate system. Away from the poles the finite difference equations are

$$\frac{\partial u}{\partial t} = \bar{z}^{\theta} \; \overline{V\cos(\theta)}^{\theta\lambda} - \frac{1}{a\cos(\theta)} \delta_{\lambda} (\phi + e) \qquad (1.9)$$

$$\frac{\partial v}{\partial t} = \bar{z}^{\lambda} \; \overline{U}^{\theta\lambda} - \frac{1}{a} \delta_{\theta} (\phi + e) \qquad (1.10)$$

$$\frac{\partial \phi}{\partial t} = - \frac{1}{a\cos(\theta)} (\delta_{\lambda} U + \delta_{\theta}(V\cos(\theta)) \qquad (1.11)$$

where the zonal and meridional mass fluxes are given by

$$U = \bar{\phi}^{\lambda} u, \quad V = \bar{\phi}^{\theta} v \quad \text{respectively}$$

and

$$e = \tfrac{1}{2}(\overline{u^2}^{\lambda} + \frac{1}{\cos(\theta)} \overline{v^2\cos(\theta)}^{\theta}), \text{ (kinetic energy)} \qquad (1.12)$$

$$z = \frac{1}{\overline{\phi\cos(\theta)}^{\theta\lambda}} \{ f\overline{\cos(\theta)}^{\theta} + \delta_{\lambda} v - \delta_{\theta}(u\cos(\theta)) \} \qquad (1.13)$$

These finite difference equations are used with the regular staggered C grid illustrated in figure (1.2), in which the dependent variables ϕ and u are kept at the poles. The finite difference scheme comprising (1.15) to (1.17) conserves the total mass, the vorticity and the potential

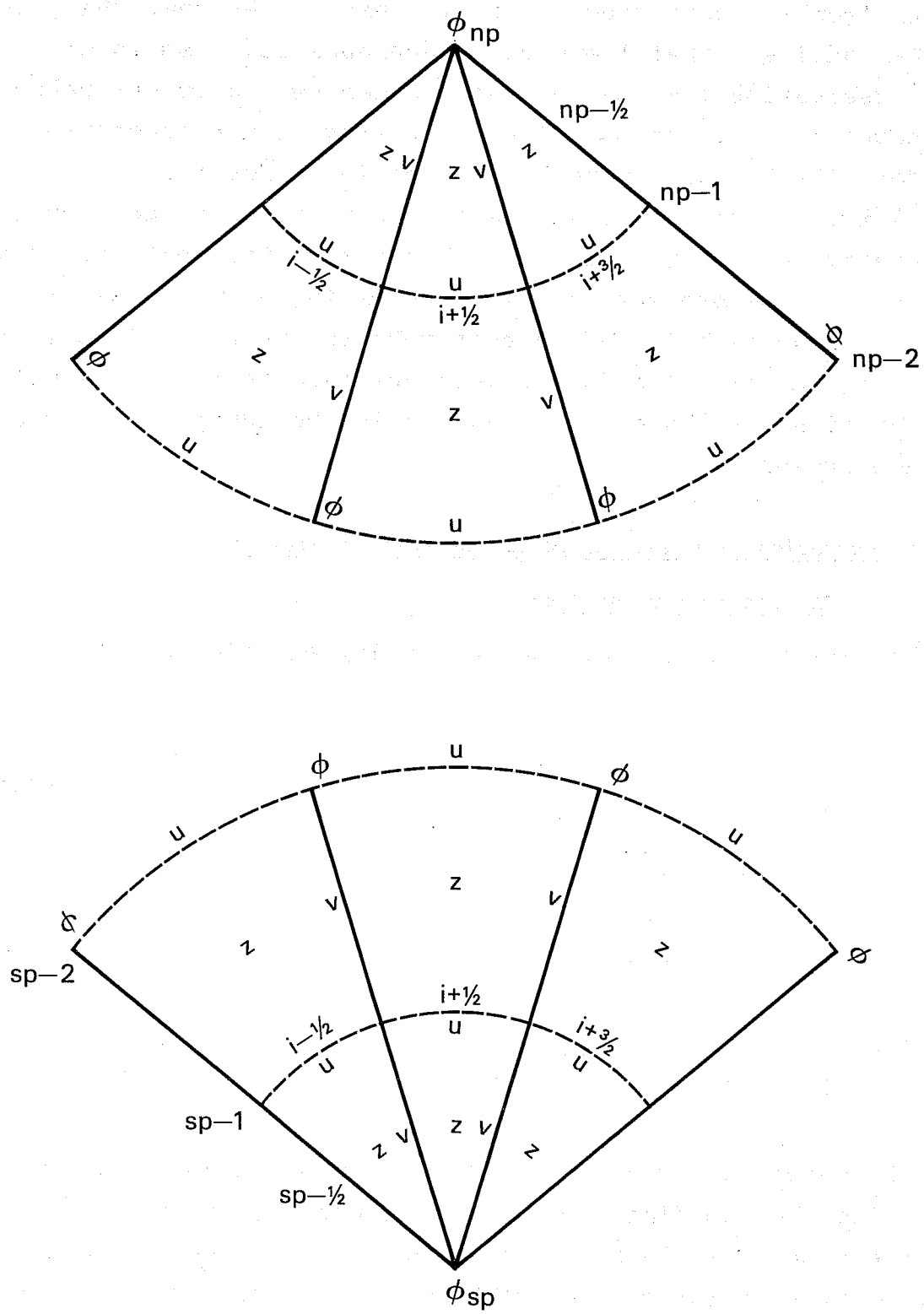

Fig. 1.2 Distribution of variables at and near the poles, np-North pole, sp-South pole.

enstrophy, apart from boundary fluxes at or near the poles. We shall see that the strict adherence to these three conservation laws can be used to derive consistent polar boundary conditions. Although energy is not conserved formally by our finite difference forms for the rotation terms, in practise it turns out that the model conserves energy very accurately. It should be noted that the work done by the pressure gradient terms in the momentum equations is balanced correctly by the increase in potential energy arising from the divergence term in the continuity equation, provided appropriate polar boundary conditions are chosen.

Conservation laws and the polar boundary conditions

(i) The continuity equation

The invariant form of the continuity equation may be written

$$\frac{\partial \phi}{\partial t} + \mathrm{div}(U,V) = 0 \qquad (1.20)$$

$$U = \phi u, \quad V = \phi u.$$

Integration over an area A gives

$$\int_A \frac{\partial \phi}{\partial t}\, dA + \int_A \mathrm{div}\,(U,V)\, dA \quad . \qquad (1.21)$$

The second integral can be turned into a line integral using the two dimensional form of Green's theorem. If the area A is the North polar cap, $\theta > \frac{\pi}{2} - \frac{\Delta\theta}{2}$, then using a finite difference analogue of Green's theorem we have

$$\sum_{i=1}^{NLON} \frac{\partial \phi}{\partial t}_{np}\, dA_p - \sum_{i=1}^{NLON} V_{np-\frac{1}{2},i} \{ a\Delta\lambda\cos(\theta_{np-\frac{1}{2}}) \} \qquad (1.22)$$

$$dA_p = \tfrac{1}{2} a\Delta\lambda\cos(\theta_{np-\frac{1}{2}})\, \frac{\Delta\theta}{2} \quad , \quad \theta_{np-\frac{1}{2}} = \frac{\pi}{2} - \frac{\Delta\theta}{2}$$

(see figure 1.2) (there are NLON points around each latitude circle). Since ϕ_{np} is independent of i, (1.22) may be rewritten as

$$NLON\frac{\partial\phi_{np}}{\partial t}\frac{a\Delta\lambda}{2}\cos(\theta_{np-\frac{1}{2}})\frac{a\Delta\theta}{2} - \sum_{i=1}^{NLON} V_{np-\frac{1}{2},i}\, a\Delta\lambda\cos(\theta_{np-\frac{1}{2}}) = 0 \qquad (1.23)$$

For the south pole we have

$$NLON\frac{\partial\phi_{sp}}{\partial t}\frac{a\Delta\lambda}{2}\cos(\theta_{sp-\frac{1}{2}})\frac{a\Delta\theta}{2} + \sum_{i=1}^{NLON} V_{sp-\frac{1}{2},i}\, a\Delta\lambda\cos(\theta_{sp-\frac{1}{2}}) = 0 \qquad (1.24)$$

with $\theta_{sp-\frac{1}{2}} = -\frac{\pi}{2} + \frac{\Delta\theta}{2}$

Equations (1.23) and (1.24) are the continuity equations for the polar points, and using these forms ensures that the total mass

$$\sum''_{\phi} \phi a^2\cos(\theta)\Delta\lambda\Delta\theta \quad \text{is conserved,}$$

provided we interpret $\cos(\theta_{np})$ as $\frac{1}{2}\cos(\theta_{np-\frac{1}{2}})$ and $\cos(\theta_{sp-\frac{1}{2}})$ as $\frac{1}{2}\cos(\theta_{sp-\frac{1}{2}})$; the sum is taken over all ϕ points (the poles are counted NLON times) and the double prime means that a factor of $\frac{1}{2}$ is applied to the contributions from polar points.

(ii) Kinetic energy generation and the form of the kinetic energy density near the poles

In order to form the kinetic energy equation we first consider sums

$$\sum_{sp-1}^{np-1}{}_{u} \bar{\phi}^{\lambda}u\,\frac{\partial u}{\partial t}\, a^2\cos(\theta)\Delta\lambda\Delta\theta \quad \text{and} \quad \sum_{v} \bar{\phi}^{\theta}v\,\cos(\theta)\frac{\partial v}{\partial t}a^2\Delta\lambda\Delta\theta;$$

$\sum_{sp-1}^{np-1}{}_{u}$ is a sum over all u points excluding the poles and

$\sum_v$ is a sum over all v points

Now

$$\sum_{\substack{u \\ sp-1}}^{np-1} \bar{\phi}^{\lambda} \frac{\partial u}{\partial t} a^2\cos(\theta)\Delta\lambda\Delta\theta = \sum_{\substack{u \\ sp-1}}^{np-1} \bar{\phi}^{\lambda} \frac{\partial}{\partial t}(\frac{u^2}{2})a^2\cos(\theta)\Delta\lambda\Delta\theta$$

$$= \sum_{\substack{\phi \\ sp-1}}^{np-1} \phi \frac{\partial}{\partial t}(\overline{\frac{u^2}{2}}^{\lambda})a^2\cos(\theta)\Delta\lambda\Delta\theta \ ,$$

and $\sum_v \bar{\phi}^{\theta} v\cos(\theta) \frac{\partial v}{\partial t} a^2\Delta\lambda\Delta\theta = \sum_v \bar{\phi}^{\theta} \frac{\partial}{\partial t}(\frac{v^2\cos(\theta)}{2})a^2\Delta\lambda\Delta\theta$

$$= \tfrac{1}{2}\phi_{np} \sum_{i=1}^{NLON} \frac{\partial}{\partial t}(\frac{v^2\cos(\theta)}{2})_{np-\frac{1}{2},i} a^2\Delta\lambda\Delta\theta +$$

$$+ \sum_{\substack{\phi \\ sp-1}}^{np-1} \phi \frac{\partial}{\partial t}(\overline{\frac{v^2\cos(\theta)}{2}}^{\theta})a^2\Delta\lambda\Delta\theta + \tfrac{1}{2}\phi_{sp} \sum_{i=1}^{NLON} \frac{\partial}{\partial t}(\frac{v^2\cos(\theta)}{2})_{sp-\frac{1}{2},i}\Delta\lambda\Delta\theta$$

Combining these two expressions gives

$$\sum_{\substack{u \\ sp-1}}^{np-1} \bar{\phi}^{\lambda} u\frac{\partial u}{\partial t}\cos(\theta)a^2\Delta\lambda\Delta\theta + \sum_v \bar{\phi}^{\theta} v\cos(\theta)\frac{\partial v}{\partial t}a^2\Delta\lambda\Delta\theta$$

$$= \tfrac{1}{2}\phi_{np} \sum_{i=1}^{NLON} \frac{\partial}{\partial t}(\frac{v^2\cos(\theta)}{2})_{np-\frac{1}{2},i} a^2\Delta\lambda\Delta\theta +$$

$$+ \sum_{\substack{\phi \\ sp-1}}^{np-1} \phi \frac{\partial}{\partial t} e \ a^2\cos(\theta)\Delta\lambda\Delta\theta +$$

$$+ \tfrac{1}{2}\phi_{sp} \sum_{i=1}^{NLON} \frac{\partial}{\partial t}(\frac{v^2\cos(\theta)}{2})_{sp-\frac{1}{2},i} a^2\Delta\lambda\Delta\theta$$

$$= \frac{\partial}{\partial t} \{ \frac{\phi_{np}}{2} \sum_{i=1}^{NLON} (\frac{v^2\cos(\theta)}{2})_{np-\frac{1}{2},i} a^2\Delta\lambda\Delta\theta \quad +$$

$$+ \sum_{sp-1}^{np-1} \phi e a^2\cos(\theta)\Delta\lambda\Delta\theta$$

$$+ \frac{\phi_{sp}}{2} \sum_{i=1}^{NLON} (\frac{v^2\cos(\theta)}{2})_{sp-\frac{1}{2}} a^2\Delta\lambda\Delta\theta \}$$

$$- \{ \frac{\partial\phi_{np}}{\partial t} \frac{1}{2} \sum_{i=1}^{NLON} (\frac{v^2\cos(\theta)}{2})_{np-\frac{1}{2}} a^2\Delta\lambda\Delta\theta \quad +$$

$$+ \sum_{sp-1}^{np-1}{}_{\phi} e\frac{\partial\phi}{\partial t} a^2\cos(\theta)\Delta\lambda\Delta\theta$$

$$\frac{\partial\phi_{sp}}{\partial t} \frac{1}{2} \sum_{i=1}^{NLON} (\frac{v^2\cos(\theta)}{2})_{sp-\frac{1}{2}} a^2\Delta\lambda\Delta\theta \quad \} \qquad (1.25)$$

The identity (1.25) shows that provided we neglect the formal lack of energy conservation in the rotation terms, the work done by the gradient forces can be balanced by a consistent conversion to potential energy provided we define

$$e_{np} = \frac{1}{\frac{1}{2}\cos(\theta_{np-\frac{1}{2}})} \frac{1}{NLON} \sum_{i=1}^{NLON} \frac{1}{2}(v^2\cos(\theta))_{np-\frac{1}{2},i}$$

and (1.26)

$$\ell_{sp} = \frac{1}{\frac{1}{2}\cos(\theta_{sp-\frac{1}{2}})} \frac{1}{NLON} \sum_{i=1}^{NLON} \frac{1}{2}(v^2\cos(\theta))_{sp-\frac{1}{2},i}$$

(iii) Conservation of vorticity and the rotation terms near the poles

By taking a finite difference CURL of the momentum equations (1.9) and (1.10) we obtain the finite difference vorticity equation

$$\frac{\partial}{\partial t}\ \{\ fa\overline{\cos(\theta)}^{\theta} + \delta_\lambda v - \delta_\theta(u\cos(\theta))\ \}\ +$$

$$+\delta_\lambda\{\ \bar{U}^{\lambda\theta}\bar{z}^{\lambda}\ \} + \delta_\theta\ \{\ \overline{V\cos(\theta)}^{\lambda\theta}\bar{z}^{\theta}\ \} = 0\ ; \qquad (1.27)$$

Note $z = \dfrac{1}{a\overline{\cos(\theta)\phi}^{\lambda\phi}}\ \{\ fa\overline{\cos(\theta)}^{\theta} + \delta_\lambda v - \delta_\theta(u\cos(\theta))\ \}$

Obviously, because (1.27) is in flux form and is valid at all z points we have vorticity conservation for arbitrary U and V. Our computations require $(\bar{U}^{\lambda\theta}\ \bar{z}^{\lambda})_{np-\frac{1}{2}}$ and $(\bar{U}^{\lambda\theta}\bar{z}^{\lambda})_{sp-\frac{1}{2}}$ which in turn needs a specification for U_{np} and U_{sp}. These "polar" mass fluxes could, of course, be derived arbitrarily by some interpolation but, in fact, the forms for U_{np} and U_{sp} can be derived by insisting that (1.27) is compatible with the finite difference continuity equation. If we set z = 1 in (1.27) we have

$$\frac{\partial}{\partial t}\ \overline{\phi a\cos(\theta)}^{\lambda\theta} + \delta_\lambda\bar{U}^{\lambda\theta} + \delta_{\bar{\theta}}\ (\overline{V\cos(\theta)}^{\lambda\theta}) = 0, \qquad (1.28)$$

and at points np-½ (1.28) becomes

$$\frac{\partial}{\partial t}\ \{\ \tfrac{1}{2}(\phi a\cos(\theta))_{np} + \tfrac{1}{2}\ (\bar{\phi}^{\lambda}_{np-1}a\cos(\theta_{np-1}))\ \}$$

$$+\ \delta_\lambda\ \{\ \tfrac{1}{2}\ \bar{U}^{\lambda}_{np} + \tfrac{1}{2}\ \bar{U}^{\lambda}_{np-1}\ \}$$

$$+\ \{\ 0-\tfrac{1}{2}\ \left[\ (\bar{V}^{\lambda}_{np-\frac{1}{2}}\cos(\theta_{np-\frac{1}{2}}) + \bar{V}^{\lambda}_{np-\frac{3}{2}}\cos(\theta_{np-\frac{3}{2}})\ \right]\ \}/\Delta\theta$$

$$= 0\ . \qquad (1.29)$$

Using the continuity equation at the points on row np-1 we may re-write (1.29) as

$$\frac{\partial}{\partial t}\ (\phi\cos(\theta))_{np} + \frac{1}{a}\delta_\lambda\bar{U}^{\lambda}_{np} - \frac{1}{a\frac{\Delta\theta}{2}}\bar{V}^{\lambda}_{np-\frac{1}{2}}\cos(\theta_{np-\frac{1}{2}}) = 0 \qquad (1.30)$$

Comparing (1.30) with (1.23) and noting that $\cos(\theta_{np})=\frac{1}{2}\cos(\theta_{np-\frac{1}{2}})$ we can derive the following equation for U_{np}, namely

$$(\delta_\lambda U_{np})_i - \frac{1}{\frac{\Delta\theta}{2}} V_{np-\frac{1}{2},i}\cos(\theta_{np-\frac{1}{2}}) = -\frac{1}{\frac{\Delta\theta}{2}} \frac{1}{NLON} \sum_{\ell=1}^{NLON} V_{np-\frac{1}{2},\ell}\cos(\theta_{np-\frac{1}{2}}) \tag{1.31}$$

which determines U_p up to a constant. We have chosen to add the extra condition

$$\sum_{\ell=1}^{NLON} U_{np,\ell} = 0 \tag{1.32}$$

For the south pole we have

$$(\delta_\lambda U_{sp})_i + \frac{1}{\frac{\Delta\theta}{2}} V_{sp-\frac{1}{2},i}\cos(\theta_{sp-\frac{1}{2}}) = \frac{1}{\frac{\Delta\theta}{2}} \frac{1}{NLON} \sum_{\ell=1}^{NLON} V_{sp-\frac{1}{2},\ell}\cos(\theta_{sp-\frac{1}{2}}) \tag{1.33}$$

and

$$\sum_{\ell=1}^{NLON} U_{sp,\ell} = 0. \tag{1.34}$$

(iv) Potential enstrophy conservation

With our choices for U_{np} and U_{sp} it is easy to show that the continuity equations and the flux equation (1.27) may be combined to arrive at the conservation law

$$\frac{\partial}{\partial t}(\overline{\phi a\cos(\theta)}^{\lambda\theta} z^2) + \delta_\lambda(\bar{U}^{\lambda\theta}\tilde{z}^{2\lambda}) + \delta_\theta(\overline{V\cos(\theta)}^{\lambda\theta}\tilde{z}^{2\theta}) = 0 \tag{1.35}$$

for the potential enstrophy $\overline{\phi a\cos(\theta)}^{\lambda\theta} z^2$,

where $(\tilde{z^2}^{\lambda})_{\lambda+\frac{\Delta\lambda}{2}} = z(\lambda+\Delta\lambda,\theta)z(\lambda,\theta)$

and $(\tilde{z^2}^{\theta})_{\theta+\frac{\Delta\theta}{2}} = z(\lambda,\theta+\Delta\theta)z(\lambda,\theta).$

1.3 Integrations on a sphere

One of the first technical difficulties that has to be overcome for global grid point models using spherical coordinate systems is the computational constraints imposed by the convergence of the meridians to the poles. A great variety of techniques have been used to overcome this problem which have met with varying degrees of success. The Kurihara (1965) grid, which is a non-uniform grid giving an almost equal area representation over the globe, has been used by Kurihara and Holloway (1967). The problems with this grid are well known (see for example Holloway and Manabe, 1971, and Holloway et al., 1973), the development of excessive high pressure calls near the poles being the main deficiency. The use of a regular latitude/longitude grid to overcome this particular problem necessitates using excessively small time-steps with explicit time-stepping schemes in order to prevent linear computational instability. Grimmer and Shaw (1967) used this grid with a time-step that is a function of latitude and they were able to use quite large time-steps except near the poles. The most favoured approach, particularly with a regular latitude/longitude grid, in recent years has been to filter out or dampen the amplitudes of short scale features near the poles or to reduce high frequencies by filtering. Mintz and Arakawa (Gates et al., 1971) used weighted averaging of the zonal pressure gradient and zonal mass flux terms in the model equations, with the degree of filtering increasing towards the poles. Holloway et al. (1973) have successfully used a regular latitude/longitude grid with Fourier chopping on all variables at the end of each time-step. Holloway et al's integrations with this approach were certainly superior to those performed on a modified Kurihara grid.

The filtering techniques that we have adopted are based on the scheme described by Arakawa and Lamb (1977), in which

they selectively applied a latitudinally dependent linear filtering operator to the longitudinal derivatives in the terms involving gravity wave propagation and also, in order to maintain energy conservation, to some parts of the non-linear advection terms. Their use of this particular filter increasingly reduces the phase speeds of small scale gravity waves as the poles are approached, rather than simply dampening amplitudes or removing short waves. This phase speed reduction enables much longer time-steps to be taken than would otherwise be allowed by the linear computational stability criterion for the unfiltered equations. The Arakawa-Lamb filter, $\underline{\underline{\mathcal{F}}}$, can be formally expressed as

$$\underline{\underline{\mathcal{F}}} = \underline{\underline{\Phi}}^{-1} \, \underline{\underline{\Lambda}} \, \underline{\underline{\Phi}} \tag{1.36}$$

where $\underline{\underline{\Phi}}$ is a finite Fourier transform of grid point values along a line of latitude, $\underline{\underline{\Phi}}^{-1}$ its inverse and

$$\underline{\underline{\Lambda}} = \underline{\underline{\Lambda}}(\theta) = \text{diag} \{ \Lambda_k(\theta), \ldots\ldots, \Lambda_{\frac{NLON}{2}}(\theta) \} \tag{1.37}$$

where $\Lambda_k^{(\theta)}$ is the reduction factor for the k^{th} Fourier mode of the term being filtered. The operator for 'Fourier chopping' can also be written in the form of (3.1), with $\underline{\underline{\Lambda}}$ having some zero elements.

For the barotropic integrations discussed in this lecture I have applied the Arakawa filter to all terms in the equations (total tendency filtering) and I have chosen

$$\Lambda_k(\theta) = \text{minimum} \left\{ \frac{\cos(\theta)}{\cos(\frac{\pi}{4})} \frac{1}{\sin(k\frac{\Delta\lambda}{2})} \, , \, 1 \right\} \tag{1.38}$$

$$k = 1, \ldots, NLON/2.$$

This choice for $\Lambda_k(\theta)$ ensures that the maximum response of the operator $\frac{1}{\cos(\theta)}\delta_\lambda$ occurs for the two grid length wave,

$k = \frac{NLON}{2}$, at the latitudes $\theta = \pm \pi/4$.

In order to test the performance of the model and the filtering scheme an N32 version, $\Delta\lambda=\Delta\theta=\frac{360}{128}=2.8125^{o}$, was integrated to 10 days with and without filtering. Two sets of initial conditions were chosen, namely, Rossby-Haurwitz wavenumbers 4 and 1. Wave number 1 providing the very important test of strong flow across the poles. The initial winds were determined from the analytic stream function using the model's finite difference scheme and balanced heights were obtained by solving the reverse balance equation. The mean geopotential height for both initial states was $7.84 \times 10^{4} m^{2} s^{-2}$. The filtered and unfiltered models were integrated with the leapfrog time-stepping scheme; no other space or time filters were used to suppress computational modes. For all the unfiltered integrations a time-step of 20 seconds was used, whereas for the filtered integrations a time-step of 240 seconds was used for the wave number-4 tests and a 180 second time-step was used for the wave number-1 tests.

The initial data for the two initial states are shown in figures (1.3) and (1.4). The unfiltered (labelled CONTROL) and filtered (labelled FILTERED) forecasts of the geopotential for day-10 are compared in figures (1.5) and (1.6) for the wave number-4 tests and in figures (1.7) and (1.8) for the wave number-1 tests. Obviously, the unfiltered and filtered integrations compare very accurately with each other, and very little difference can be discerned either visually or objectively. The unfiltered and filtered zonal mean geopotentials day-10 are plotted against latitude in figure (1.9) for the wavenumber-4 integrations, and in figure (1.10) for the wavenumber-1 integrations. Both forecasts are identical in this aspect and obviously there is no evidence of spurious rising heights near or at the poles.

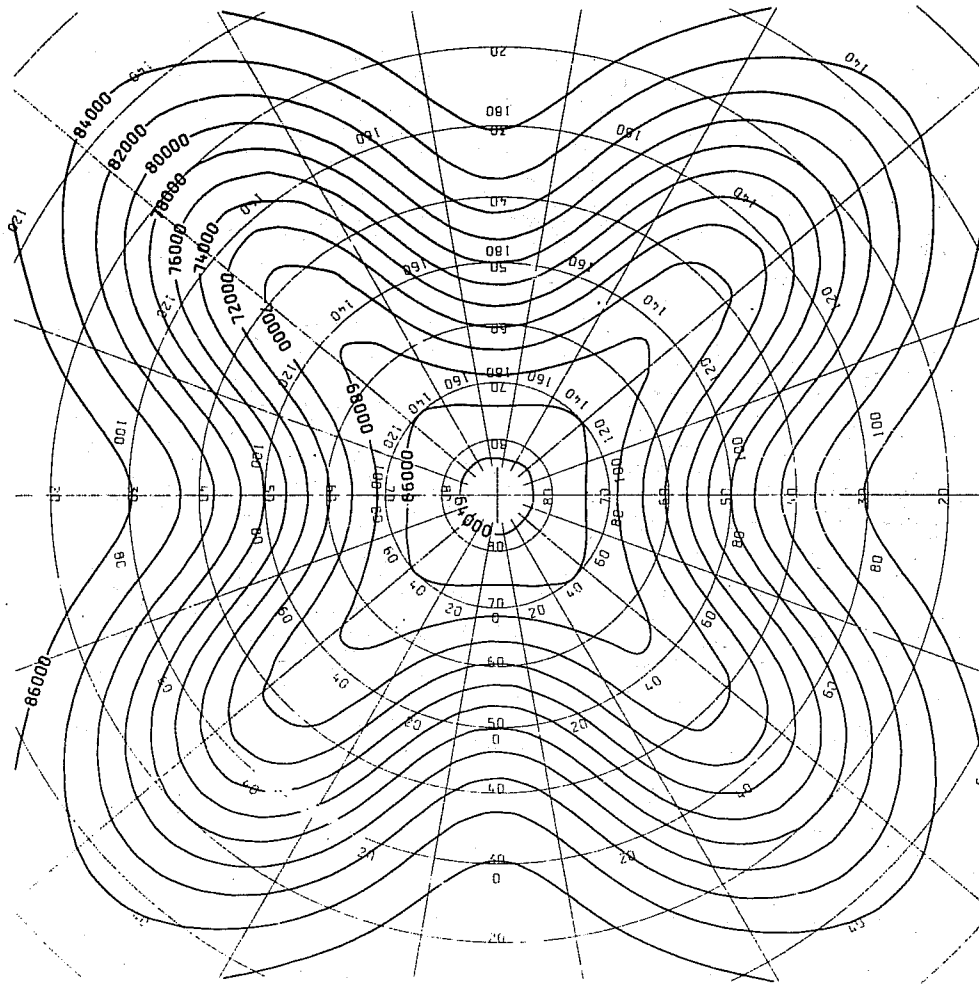

Fig. 1.3 Rossby Haurwitz wave number 4 test initial data

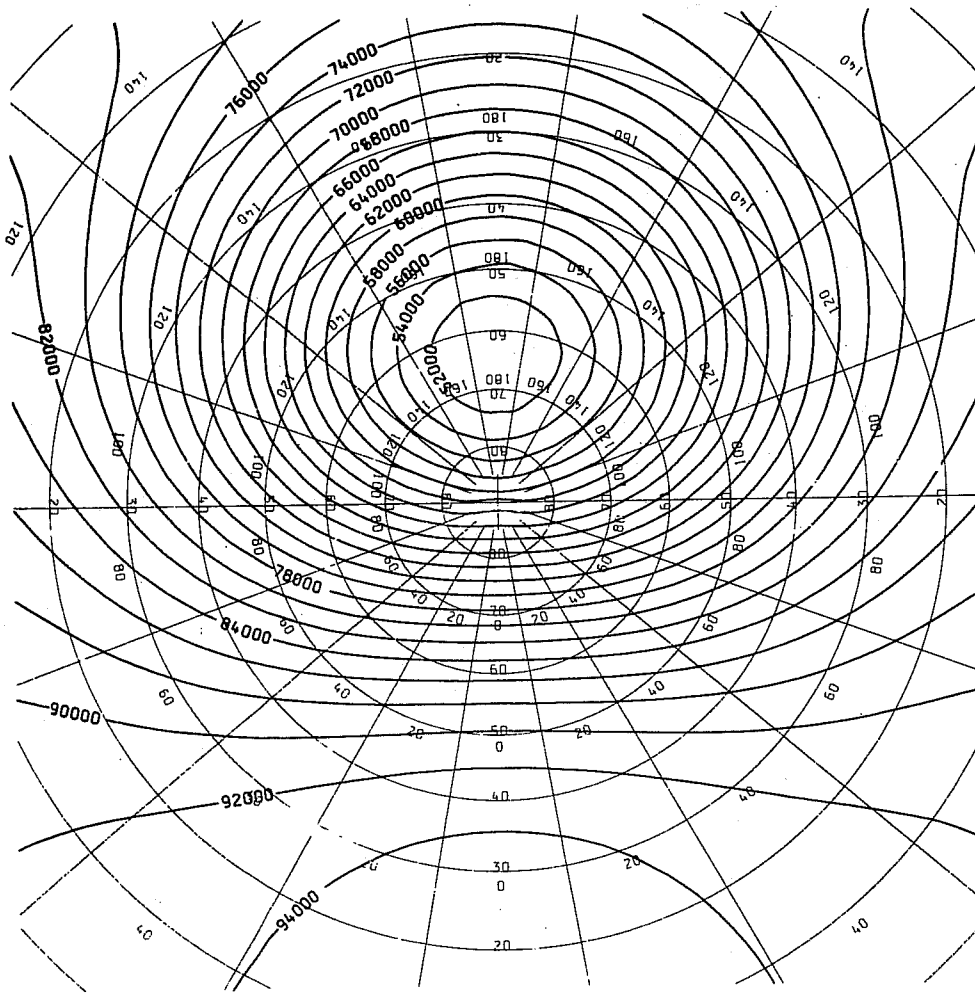

Fig. 1.4 Rossby Haurwitz wave number 1 test initial data.

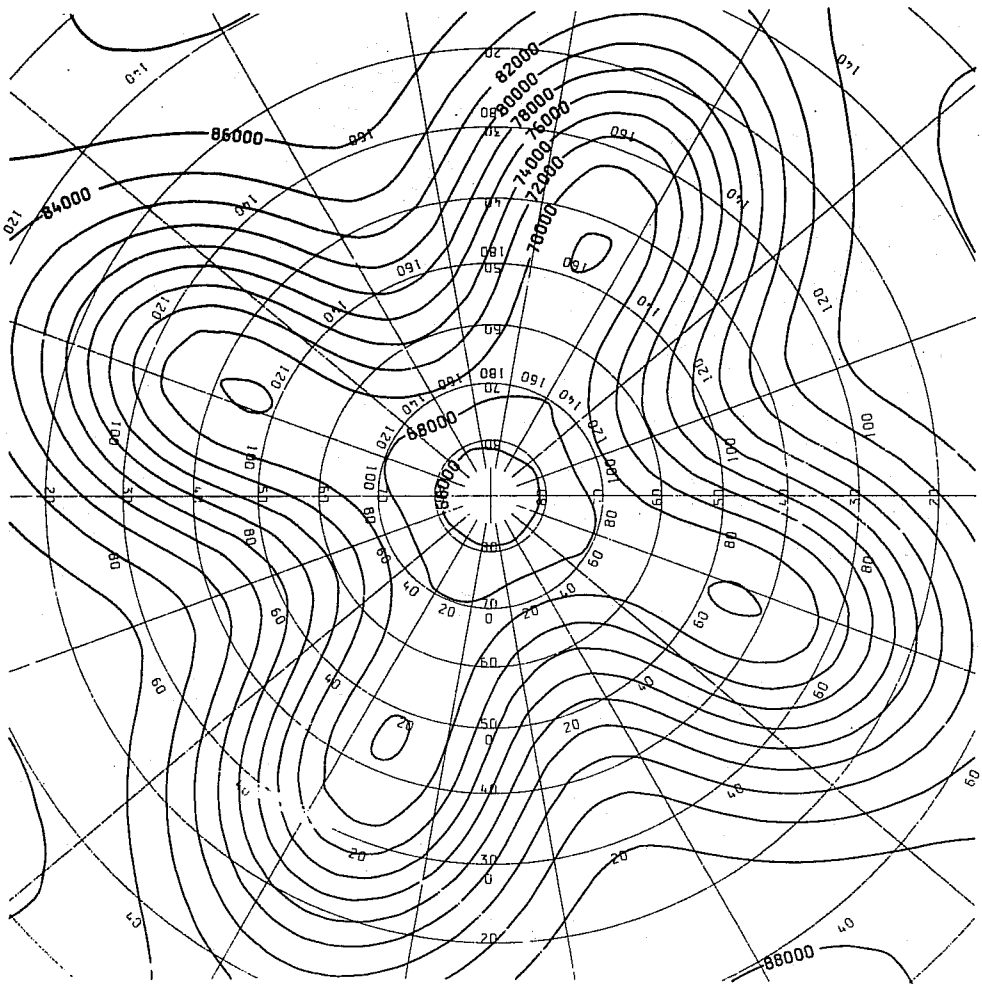

Fig. 1.5 Rossby Haurwitz wave number 4 test, day - 10 (CONTROL)

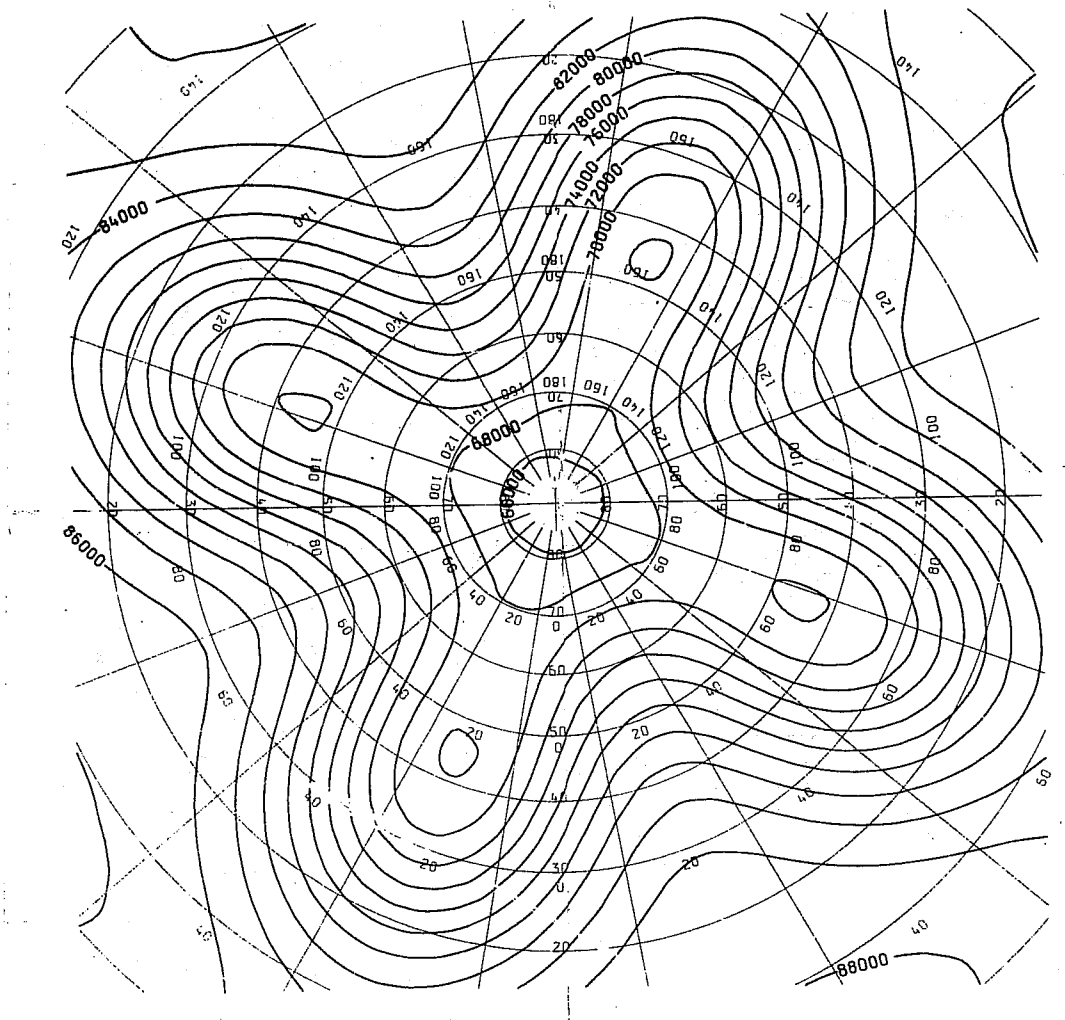

Fig. 1.6 Rossby Haurwitz wave number 4 test, day - 10 (FILTERED)

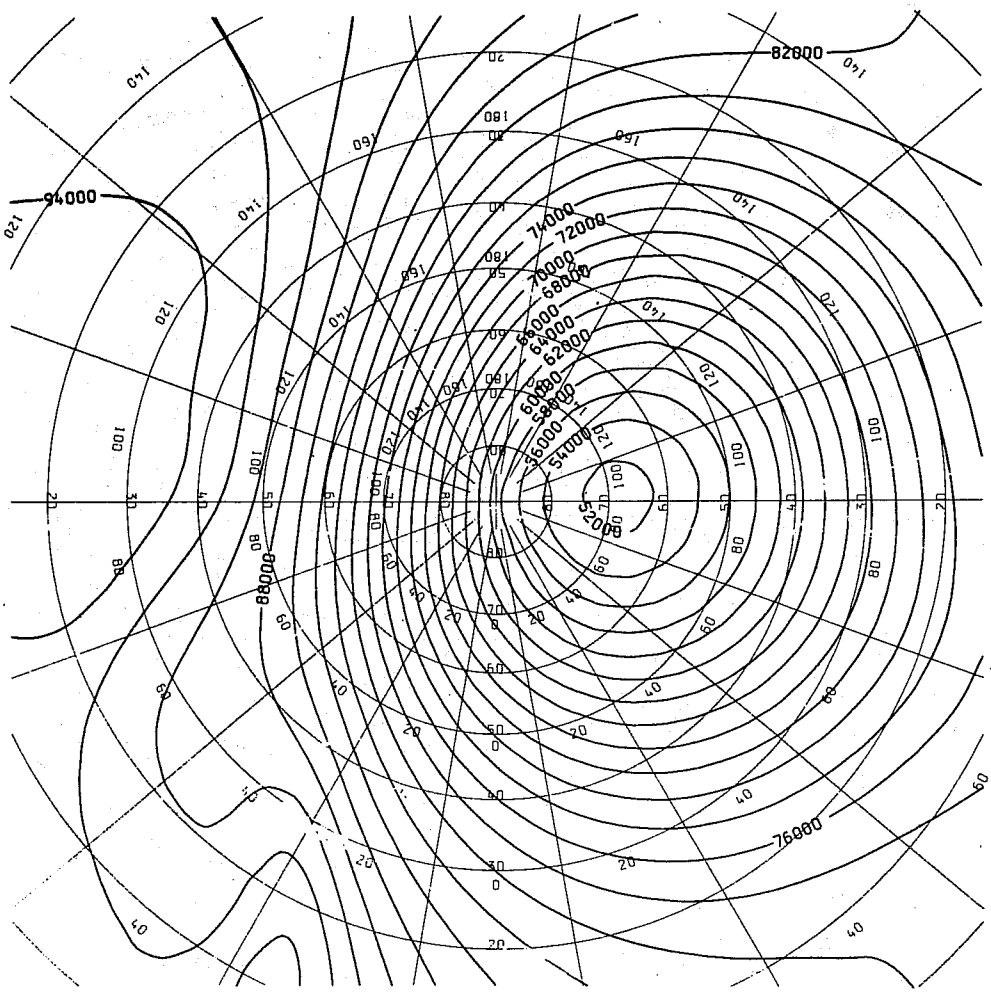

Fig. 1.7 Rossby Haurwitz wave number 1 test, day - 10 (CONTROL)

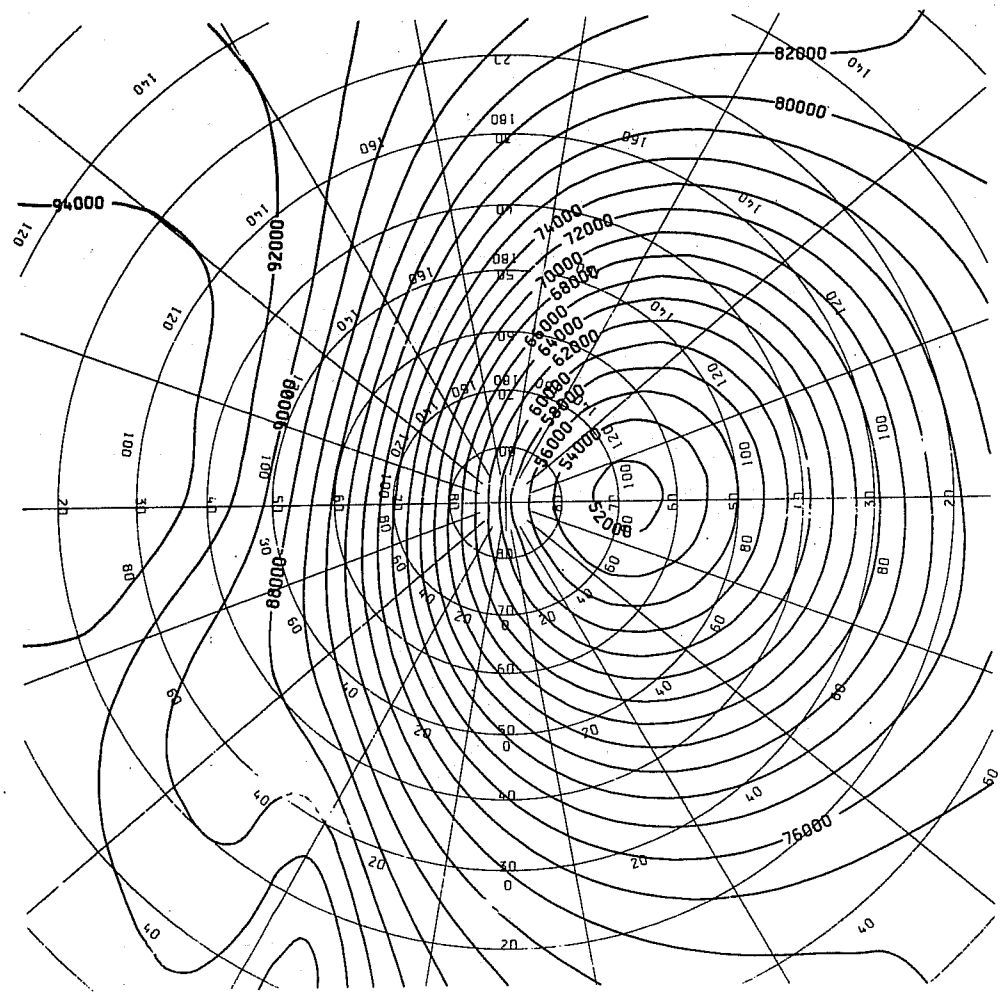

Fig. 1.8 Rossby Haurwitz wave number 1 test, day - 10 (FILTERED)

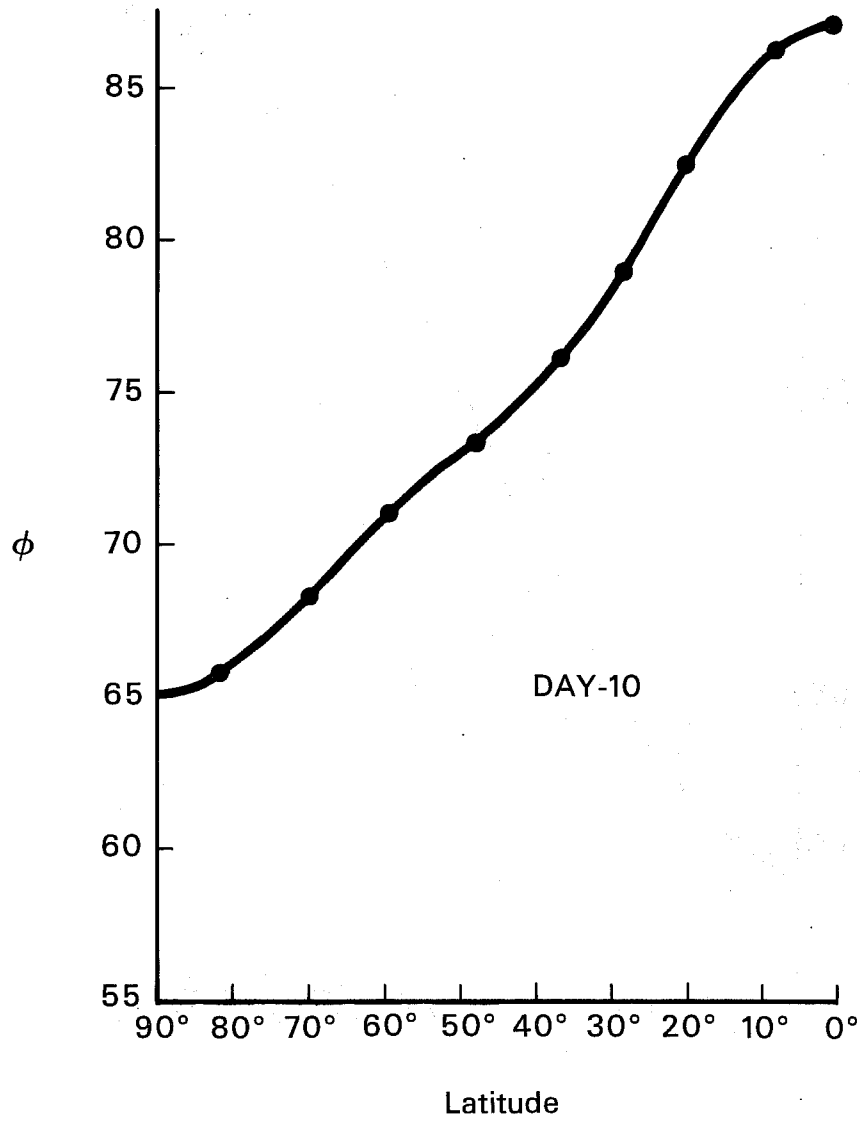

Fig. 1.9 Zonal mean geopotential versus latitude. Control - solid line, Filtered run - dots, Rossby Haurwitz wave - 4.

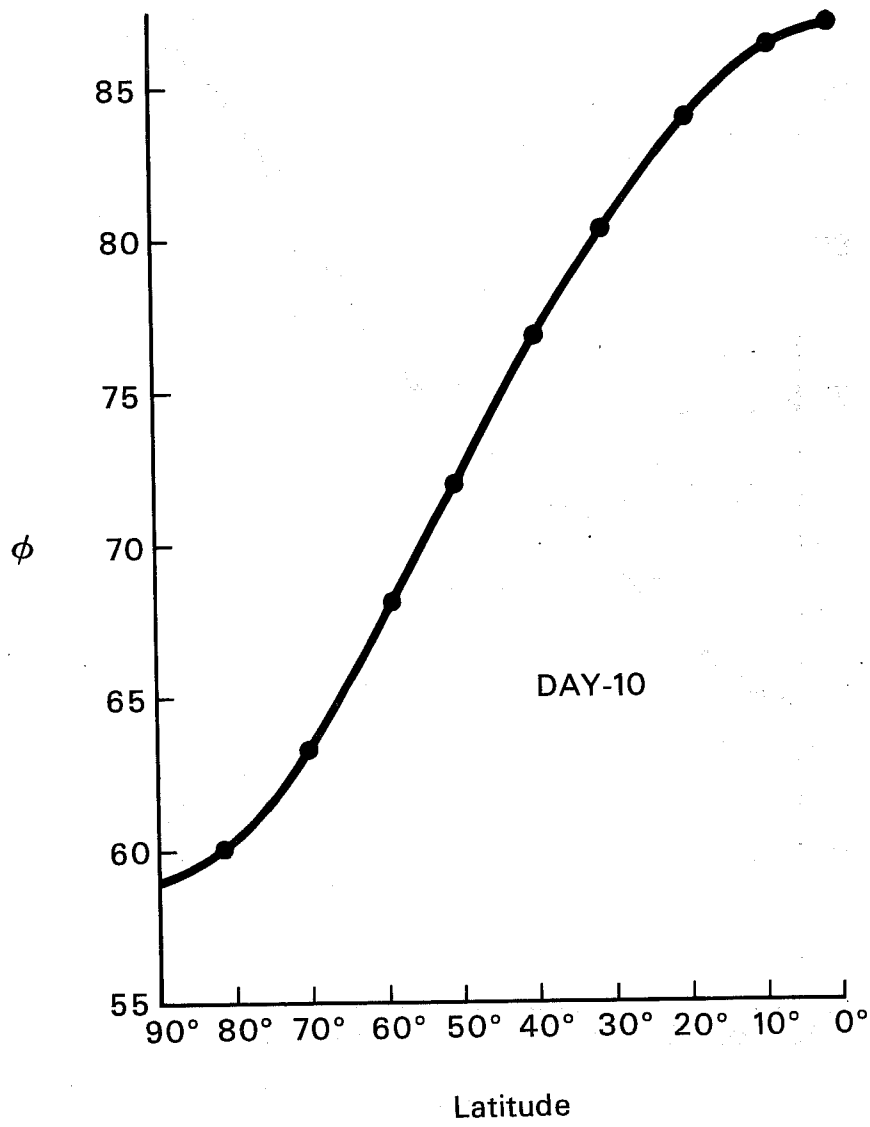

Fig. 1.10 Zonal mean geopotential versus latitude. Control - solid line, Filtered run - dots. Rossby Haurwitz wave - 1.

2. VERTICAL DIFFERENCING SCHEMES FOR BAROCLINIC PRIMITIVE EQUATION MODELS

In this lecture I shall discuss the methodology underlying the design of the centres vertical differencing scheme. The approach is again based on the imposition of some important conservation laws.

2.1 Governing equations

The equations for a dry adiabatic version of our model are

$$\frac{\partial p_s}{\partial t} + \nabla_\sigma \cdot (p_s \underline{v}) + \frac{\partial}{\partial \sigma}(p_s \dot{\sigma}) = 0, \quad \text{conservation of mass,} \tag{2.1}$$

$$\frac{\partial \underline{v}}{\partial t} + Z\, \underline{k} \wedge \underline{v} + \dot{\sigma} \frac{\partial \underline{v}}{\partial \sigma} + \nabla_\sigma(\phi + e) + RT\nabla_\sigma \ell n p_s = 0$$

momentum, (2.2)

$$p_s \frac{\partial T}{\partial t} + p_s \underline{v} . \nabla_\sigma T + p_s \dot{\sigma} \frac{\partial T}{\partial \sigma} - \frac{\kappa T \omega}{\sigma} = 0,$$

aliter

$$\frac{\partial}{\partial t}(p_s C_p T) + \nabla_\sigma . (p_s \underline{v} C_p T) + \frac{\partial}{\partial \sigma}(p_s \dot{\sigma} C_p T) - \frac{RT\omega}{\sigma} = 0$$

thermodynamics, (2.3)

$$\frac{\partial \phi}{\partial \ell n \sigma} = - RT \qquad \text{(hydrostatic equation);} \tag{2.4}$$

the vertical coordinate is σ and is defined by

$$\sigma = p/p_s, \tag{2.5}$$

$$Z = \frac{1}{p_s} f + \frac{1}{a\cos(\theta)} \left(\frac{\partial v}{\partial \lambda} - \frac{\partial}{\partial \theta}(a\cos(\theta)) \right),$$

$$e = \tfrac{1}{2}(u^2 + v^2) = \tfrac{1}{2} \underline{v} . \underline{v},$$

$$\omega = \dot{p} = p_s \sigma + \sigma \{ \frac{\partial p_s}{\partial t} + \underline{v} . \nabla_\sigma p_s \}$$

In order to complete the system we require upper and lower boundary conditions; we have selected the "no flux" conditions

$$\left.\begin{aligned} (p_s\dot{\sigma})_{\sigma=0} &= 0 \\ \text{and} \\ (p_s\sigma)_{\sigma=1} &= 0 \quad . \end{aligned}\right\} \qquad (2.6)$$

For our model we required mass and energy conservation. In particular, we wanted the work done by pressure forces to be balanced by the changes in the total potential energy arising from $\frac{RT\omega}{\sigma}$, the ω-term.

Integration of the continuity equation gives

$$\frac{\partial p_s}{\partial t} = -\int_0^1 \nabla_\sigma.(p_s\underline{v})d\sigma - \left[p_s\dot{\sigma}\right]_0^1 = -\nabla_\sigma.\int_0^1 p_s\underline{v}d\sigma. \qquad (2.7)$$

The divergence term in (2.7) integrates to zero over the globe, which means that the total mass is conserved.

A "kinetic energy" equation can be derived from the momentum equations in the form

$$p_s\underline{v}.\frac{\partial \underline{v}}{\partial t} + p_s\dot{\sigma}\underline{v}.\frac{\partial \underline{v}}{\partial \sigma} + p_s\underline{v}.\nabla_\sigma e + p_s\underline{v}.(\nabla_\sigma\phi+RT\nabla_\sigma \ell np_s) = 0$$

or

$$p_s\frac{\partial e}{\partial t} + p_s\underline{v}.\nabla_\sigma e + p_s\dot{\sigma}\frac{\partial e}{\partial \sigma} + p_s\underline{v}.(\nabla_\sigma\phi+RT\nabla_\sigma \ell np_s) = 0 \qquad (2.8)$$

Using the continuity equation, (2.1), (2.8) may be rewritten as

$$\frac{\partial}{\partial t}(p_s e) + \boxed{\nabla_\sigma(p_s\underline{v}e) + \frac{\partial}{\partial\sigma}(p_s\dot{\sigma}e)} + p_s\underline{v}.(\nabla_\sigma\phi+RT\nabla_\sigma \ell np_s) = 0 \qquad (2.9)$$

In order to construct the total energy equation we need to express the pressure gradient terms in another form. Using the continuity and hydrostatic equations we have

$$p_s \underline{v}.\nabla_\sigma \phi = \nabla_{\dot\sigma}(p_s \underline{v}\phi) - \phi\, \nabla_\sigma . p_s \underline{v}$$

$$= \nabla_{\dot\sigma}(p_s \underline{v}\phi) + \phi\left(\frac{\partial p_s}{\partial t} + \frac{\partial}{\partial \sigma}(p_s \dot\sigma)\right)$$

$$= \nabla_{\dot\sigma}(p_s \underline{v}\phi) + \frac{\partial}{\partial \sigma}\left(\phi\left(\sigma \frac{\partial p_s}{\partial t} + p_s \dot\sigma\right)\right) - \frac{\partial \phi}{\partial \sigma}\left(\sigma \frac{\partial p_s}{\partial t} + p_s \dot\sigma\right) \tag{2.10}$$

Combining (2.9) and (2.10) we have

$$\frac{\partial (p_s e)}{\partial t} + \boxed{\nabla_{\sigma_o}(p_s \underline{v} e) + \frac{\partial}{\partial \sigma}(p_s \dot\sigma e) + \nabla_\sigma (p_s \underline{v}\phi) + \frac{\partial}{\partial \sigma}\left(\sigma \frac{\partial p_s}{\partial t} + p_s \dot\sigma\right)\phi} - \frac{\partial \phi}{\partial \sigma}\left\{ \sigma \frac{\partial p_s}{\partial t} + p_s \dot\sigma \right\} + RT p_s \underline{v}.\nabla_\sigma \ell n p_s = 0$$

Now

$$- \frac{\partial \phi}{\partial \sigma}\left\{\sigma \frac{\partial p_s}{\partial t} + p_s \dot\sigma \right\} + RT p_s \underline{v}.\nabla_\sigma \ell n p_s$$

$$= \frac{RT}{\sigma}\left(\sigma \frac{\partial p_s}{\partial t} + p_s \dot\sigma\right) + RT \underline{v}.\nabla_\sigma p_s = \frac{RT\omega}{\sigma}$$

Addition of the kinetic energy equation and the flux form of the thermodynamic equation and integration from σ=0 to 1 gives

$$\frac{\partial}{\partial t}\left\{ p_s \phi_s + \int_o^1 p_s (e + C_p T) d\sigma \right\} + \nabla_\sigma . \int_o^1 p_s \underline{v}(e + C_p T + \phi) d_\sigma = 0 \tag{2.11}$$

Equation (2.11) is an expression of the energy conservation law for the σ system (2.1) to (2.5). The divergence term in (2.11) integrates to zero over the whole globe which

means that the total energy, potential plus kinetic, is conserved.

2.2 A finite difference scheme which maintains conservation of mass and energy

The disposition of variables and the grid structure in the vertical for the ECMWF primitive equation models is illustrated in figure (2.1). The primary variables $\underline{v}$ and T are kept at the full levels and the vertical velocity $\dot{\sigma}$ and the geopotential are kept at half levels. The variable grid spacing $\Delta\sigma_k$ is defined by

$$\Delta\sigma_k = \sigma_{k+\frac{1}{2}} - \sigma_{k-\frac{1}{2}} \tag{2.12}$$

(i) The equation of continuity

The continuity equation is taken in the form

$$\frac{\partial p_s}{\partial t} + \nabla_\sigma \cdot (p_s \underline{v}_k) + \frac{\Delta(p_s \dot{\sigma})_k}{\Delta\sigma_k} = 0 \tag{2.13}$$

Multiplying (2.13) by $\Delta\sigma_k$ and summing (integration) from $k = 1, \ldots, K$ gives

$$\sigma_{k+\frac{1}{2}} \frac{\partial p_s}{\partial t} + \sum_{k=1}^{K} \nabla_\sigma \cdot (p_s \underline{v}_k)\Delta\sigma_k + p_s \dot{\sigma}_{k+\frac{1}{2}} = 0 \tag{2.14}$$

$$(p_s \dot{\sigma}_{\frac{1}{2}} = 0)$$

For $K = N$ we have

$$\frac{\partial p_s}{\partial t} = -\sum_{k=1}^{N} \nabla_\sigma \cdot (p_s \underline{v}k)\Delta\sigma_k = -\nabla_\sigma \cdot \sum_{k=1}^{N} \nabla_\sigma (p_s \underline{v}_k)\Delta\sigma_k \tag{2.15}$$

Equation (2.15) is a finite difference analogue of (2.7) which obviously conserves the total (global) mass of the model atmosphere.

VERTICAL GRID

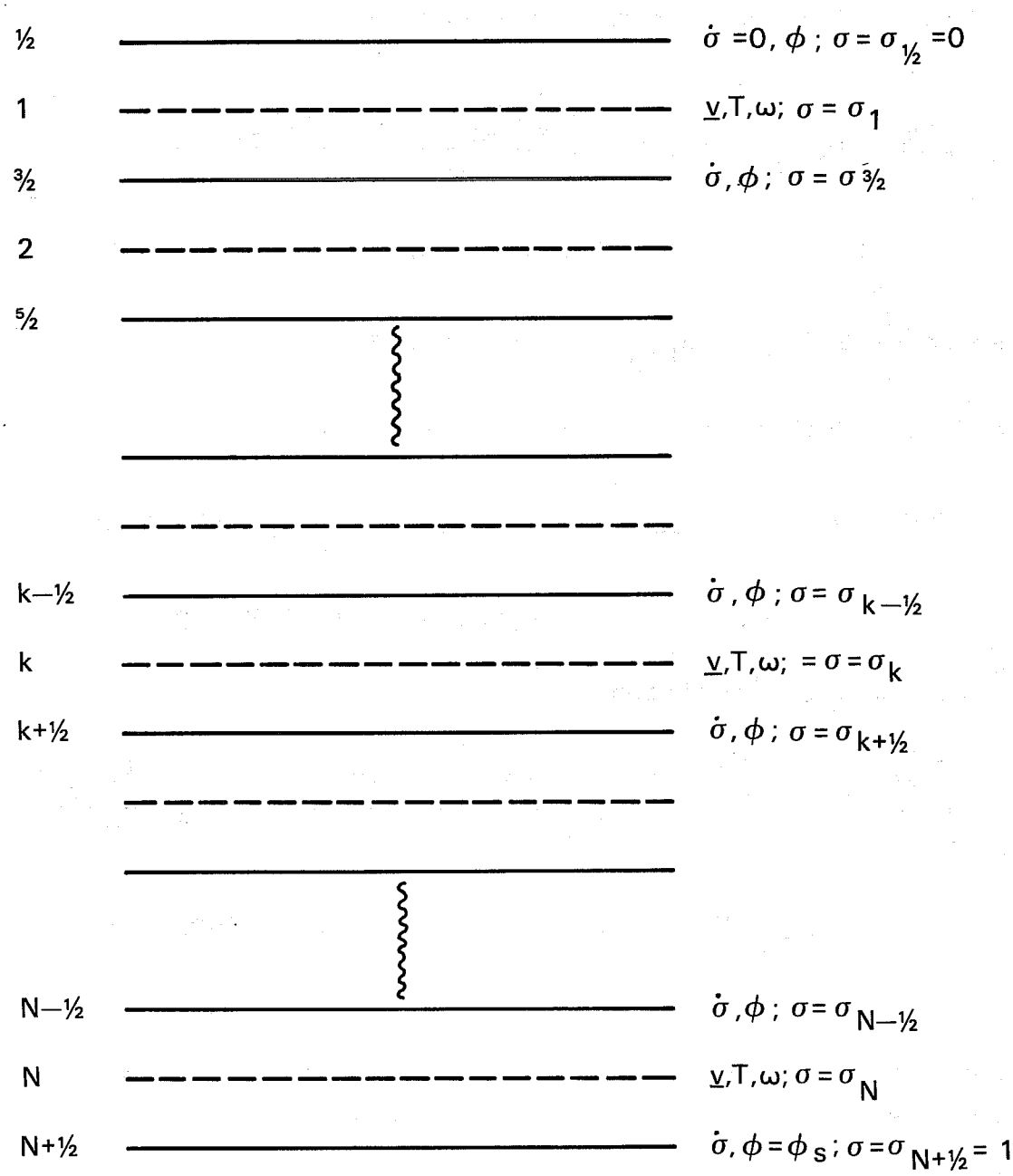

Fig. 2.1 Vertical disposition of variables.

(ii) Energy conservation

The finite difference momentum equation is

$$\frac{\partial \underline{v}_k}{\partial t} + Z\underline{k}\wedge\underline{v}_k + \tfrac{1}{2}\left\{\frac{\dot{\sigma}_{k+\frac{1}{2}}(\underline{v}_{k+1}-\underline{v}_k) + \dot{\sigma}_{k-\frac{1}{2}}(\underline{v}_k-\underline{v}_{k-1})}{\Delta_\sigma \sigma_k}\right\}$$

$$+ \nabla_\sigma \{\phi_k + e_k\} + RT_k \nabla_\sigma \ell n p_s = 0, \qquad (2.16)$$

where $\phi_k = \alpha_k \phi_{k+\frac{1}{2}} + \beta_k \phi_{k-\frac{1}{2}}$ with $\alpha_k + \beta_k = 1$.

The finite difference kinetic energy equation is

$$p_s \underline{v}_k \cdot \frac{\partial \underline{v}_k}{\partial t} + \tfrac{1}{2}\, p_s \underline{v}_k \cdot \{\dot{\sigma}_{k+\frac{1}{2}}(\underline{v}_{k+1} - \underline{v}_k) + \dot{\sigma}_{k-\frac{1}{2}}(\underline{v}_k - \underline{v}_{k-1})\}/\Delta\sigma_k$$

$$+ p_s \underline{v}_k \cdot \nabla_\sigma e_k + p_s \underline{v}_k \cdot \{\nabla_\sigma \phi_k + RT_k \nabla_\sigma \ell n p_s\} = 0,$$

and this may be rewritten as

$$p_s \frac{\partial e_k}{\partial t} + \tfrac{1}{2}\left(\frac{p_s \dot{\sigma}_{k+\frac{1}{2}} \underline{v}_{k+1}\cdot\underline{v}_k - p_s \dot{\sigma}_{k-\frac{1}{2}} \underline{v}_k \cdot \underline{v}_{k-1}}{\Delta\sigma_k}\right) - \tfrac{1}{2}\underline{v}_k \cdot \underline{v}_k \frac{\Delta(p_s\dot{\sigma})_k}{\Delta\sigma_k}$$

$$+ p_s \underline{v}_k \cdot \nabla_\sigma e_k + p_s \underline{v}_k \cdot \{\nabla_\sigma \phi_k + RT_k \nabla_\sigma \ell n p_s\} = 0 \qquad (2.17)$$

Using the finite difference continuity equation we may rewrite equation (2.17) in the flux form

$$\frac{\partial}{\partial t}(p_s e_k) + \nabla_\sigma \cdot (p_s \underline{v}_k e_k) + \Delta_\sigma\left(\frac{p_s \dot{\sigma} \tilde{\underline{v}}^{2\sigma}}{2}\right)_k + p_s \underline{v}_k \cdot \{\nabla_\sigma \phi_k + RT_k \nabla_\sigma \ell n p_s\} = 0 \qquad (2.18)$$

where $(\tilde{\underline{v}}^2)_{k+\frac{1}{2}} = \underline{v}_{k+1}\cdot\underline{v}_k$ (geometric mean).

In order to derive the analogue of the identity (2.10) we need a hydrostatic equation; we use

$$\left(\frac{\Delta_\sigma \phi}{\Delta \ell n \sigma}\right)_k = -RT_k \qquad (2.19)$$

For the finite difference model we have

$$p_s \underline{v}_k \cdot \nabla_\sigma \phi_k = \nabla_\sigma \cdot \{p_s \underline{v}_k \phi_k\} - \phi_k \nabla_\sigma \cdot (p_s \underline{v}_k)$$

$$= \nabla_\sigma \cdot \{p_s \underline{v}_k \phi_k\} + \phi_k \{\frac{\partial p_s}{\partial t} + \frac{\Delta_\sigma (p_s \dot{\sigma})_k}{\Delta \sigma_k}\}$$

$$= \nabla_\sigma \cdot \{p_s \underline{v}_k \phi_k\} + \frac{\phi_k}{\Delta \sigma_k} \Delta_\sigma (\sigma \frac{\partial p_s}{\partial t} + p_s \dot{\sigma})_k$$

$$= \nabla_\sigma \cdot (p_s \underline{v} \phi_k) + \frac{\Delta_\sigma (\phi (\sigma \frac{\partial p_s}{\partial t} + p_s \dot{\sigma}))_k}{\Delta \delta_k}$$

$$- \frac{(\Delta_\sigma \phi)_k}{\Delta \sigma_k} \left[\beta_k (\sigma \frac{\partial p_s}{\partial t} + p_s \dot{\sigma})_{k+\frac{1}{2}} + \alpha_k (\sigma \frac{\partial p_s}{\partial t} + p_s \dot{\sigma})_{k-\frac{1}{2}} \right] \qquad (2.20)$$

(Note: $\phi_k (A_{k+\frac{1}{2}} - A_{k-\frac{1}{2}}) = (\alpha_k \phi_{k+\frac{1}{2}} + \beta_k \phi_{k-\frac{1}{2}}) (\psi_{k+\frac{1}{2}} - \psi_{k-\frac{1}{2}})$

$$= (\phi_{k+\frac{1}{2}} A_{k+\frac{1}{2}} - \phi_{k-\frac{1}{2}} A_{k-\frac{1}{2}})$$

$$- (\phi_{k+\frac{1}{2}} - \phi_{k-\frac{1}{2}}) (\beta_k A_{k+\frac{1}{2}} + \alpha_k A_{k-\frac{1}{2}}).$$

If we require total energy conservation then the form of the last term in (2.20) is a constraint on our choice for the ω term, $\frac{\kappa T \omega}{\sigma}$, in the thermodynamic equation.

The thermodynamic equation for our model is

$$p_s \frac{\partial T_k}{\partial t} + p_s \underline{v}_k \cdot \nabla_\sigma T_k + p_s^{\frac{1}{2}} \left\{ \frac{\dot{\sigma}_{k+\frac{1}{2}} (T_{k+1} - T_k) + \dot{\sigma}_{k-\frac{1}{2}} (T_k - T_{k-1})}{\Delta \sigma_k} \right\} - \left[\frac{\kappa T \omega}{\sigma} \right]_k$$

$$= 0 \qquad (2.21)$$

If the ω term is chosen to maintain energy conservation we have

$$\left[\frac{\kappa T\omega}{\sigma}\right]_k = \frac{1}{C_p}\left[\frac{RT\omega}{\sigma}\right] = \frac{1}{C_p}\left[-\frac{(\Delta\phi)_k}{\Delta\sigma_k}\left\{\beta_k(\sigma\frac{\partial p_s}{\partial t} + p_s\dot{\sigma})_{k+\frac{1}{2}} + \alpha_k(\sigma\frac{\partial p_s}{\partial t} + p_s\dot{\sigma})_{k-\frac{1}{2}}\right\}\right.$$

$$\left. + RT_k\underline{v}_k.\nabla p_s\right]$$

$$= \frac{1}{C_p}\left[RT_k(\frac{\Delta\ell n\sigma}{\Delta\sigma})_k\left\{\beta_k(\sigma\frac{\partial p_s}{\partial t} + p_s\dot{\sigma})_{k+\frac{1}{2}} + \alpha_k(\sigma\frac{\partial p_s}{\partial t} + p_s\dot{\sigma})_{k-\frac{1}{2}}\right\}\right.$$

$$\left. + RT_k p_s\underline{v}_k.\nabla\ell np_s\right] \qquad (2.22)$$

The term $(\frac{\Delta\ell n\sigma}{\Delta\sigma})_k$ can be interpreted as a definition of $(\frac{1}{\sigma_k})$ for the model.

From (2.22) we note that we still have a degree of freedom remaining, namely the choice of α_k and β_k, subject to $\alpha_k + \beta_k = 1$. For our operational model we use $\alpha_k = \beta_k = \frac{1}{2}$. But these weights can be chosen in such a way that no spurious angular momentum is generated by pressure forces, Simmons (1979).

2.3 Comments on the stability of the three dimensional baroclinic model

The finite difference scheme for the centre's global grid point model is a combination of the horizontal and vertical schemes described in this lecture and lecture 1, and it is fully described in Burridge, Haseler's (1977) report. As a demonstration of the stability of the finite difference scheme, two 10-day integrations we performed with the full operational model (N48, $\Delta\lambda = \Delta\theta = 1.875^o$; 15 levels; physical parameterization as described by Tiedtke et al (1979)). The first integration (labelled R70) had no horizontal dissipation/diffusion, whereas the second (labelled R54) used a non-linear fourth order

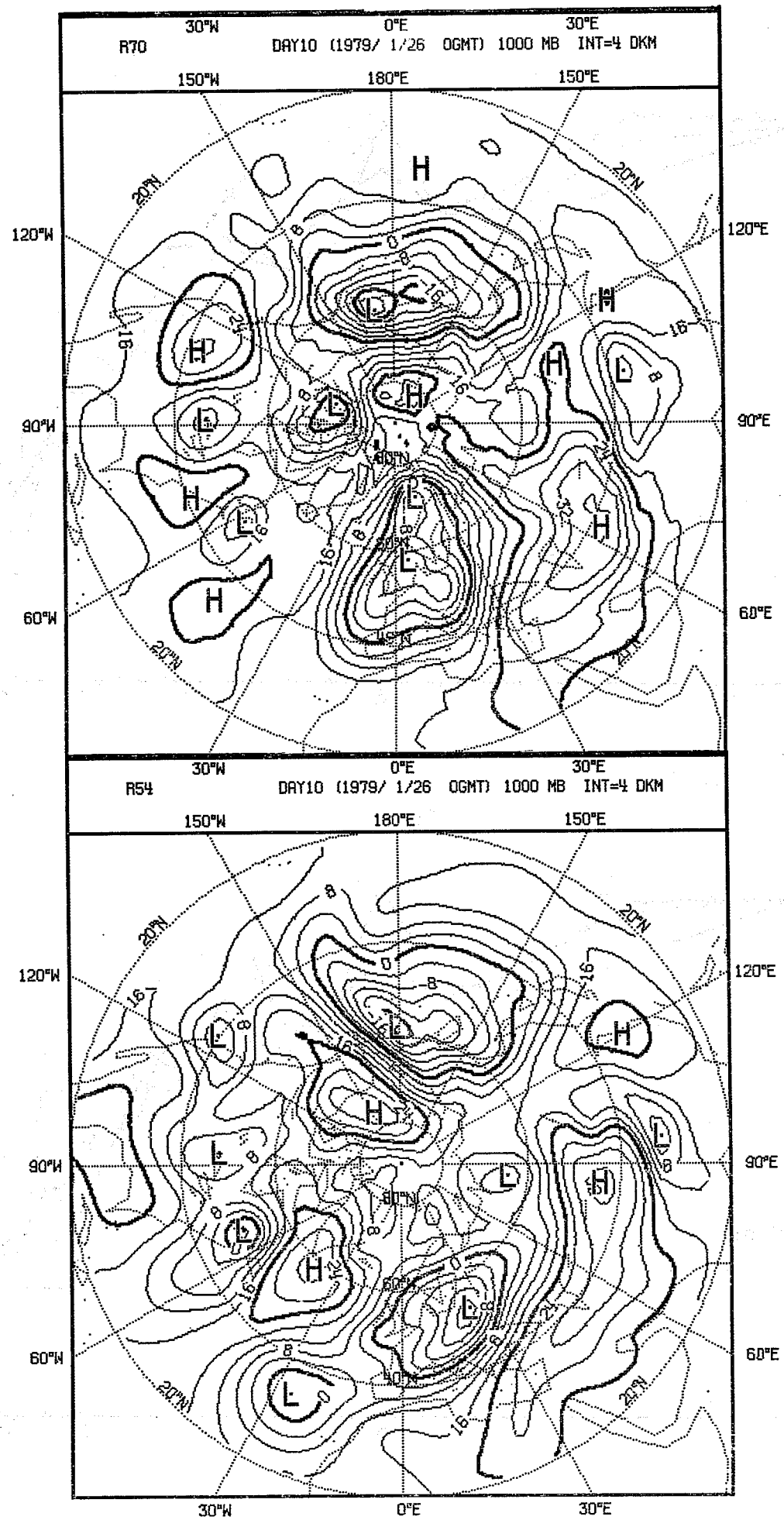

Fig. 2.2 10 day forecasts of the 1000 mb height field from the undiffused (R70) and the diffused (R54) integrations.

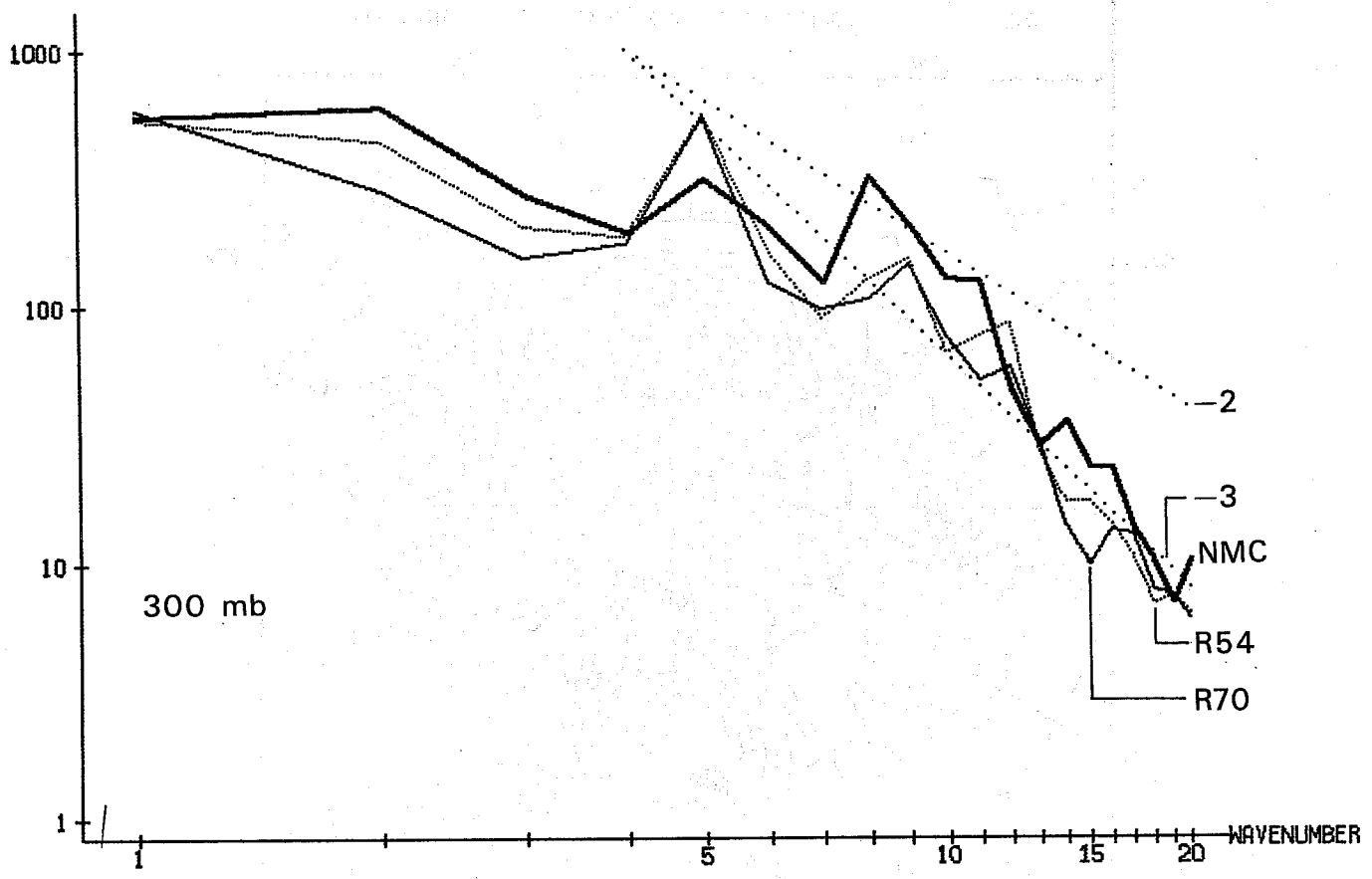

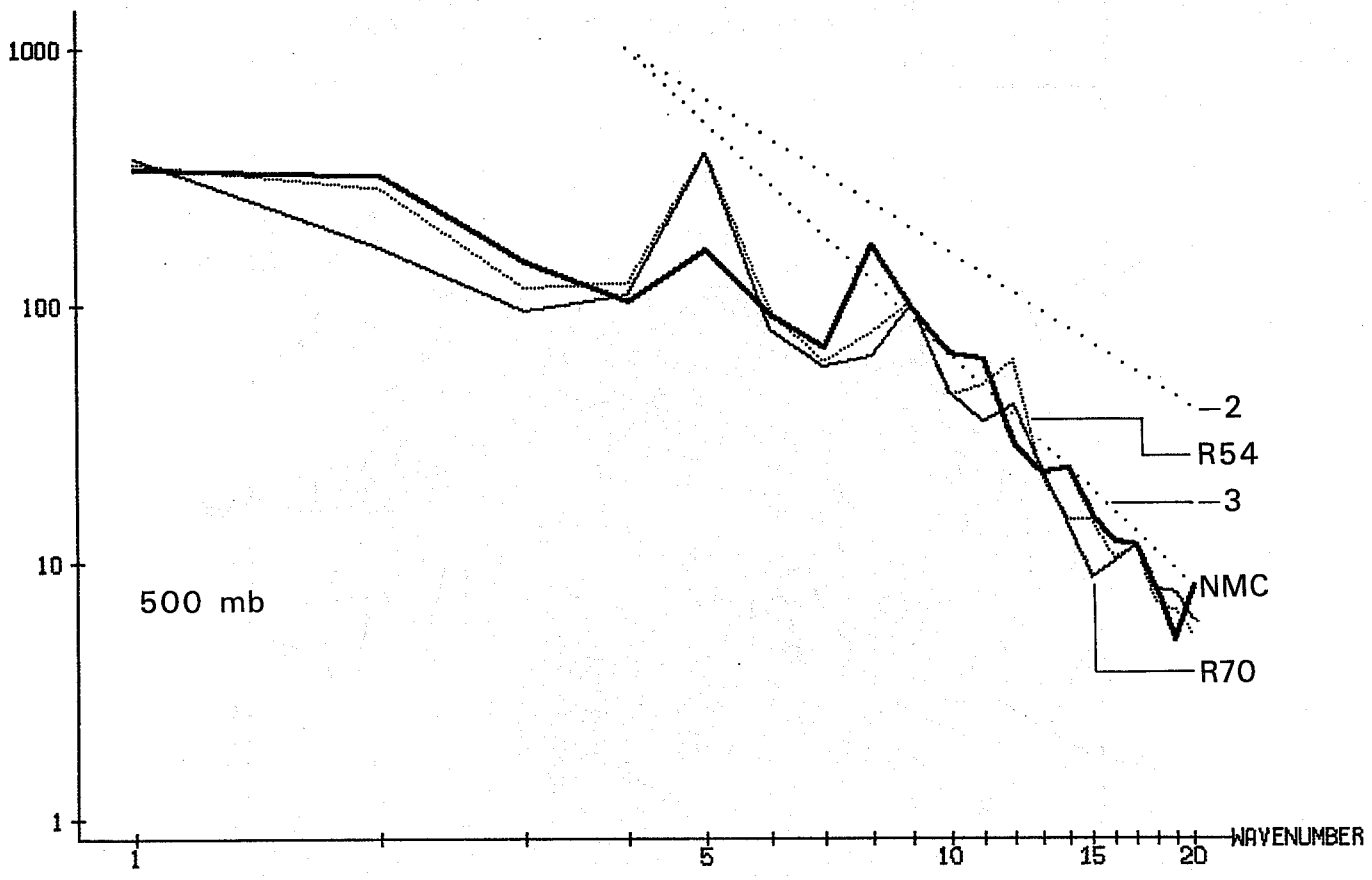

Fig. 2.3 Spectrum of kinetic energy. KJ/(M2 x BAR). Day 4.5 to 8.0. Mean between 40 and 60.

horizontal smoothing operator designed by Hollingsworth et al. (1977). The two 10-day forecasts are illustrated in figure (2.2) by 1000mb contour maps; the spectrum (up to zonal wave number 20) of kinetic energy for the two forecasts is compared with an NMC analysed spectrum in figure (2.3). The performance of the undiffused model is remarkable. My purpose in presenting this comparison is not to advocate models with little or no horizontal diffusion but simply to emphasize the stability that can be achieved by a careful choice of the finite difference scheme. In fact, objective and subjective comparisons of horizontally smoothed and unsmoothed forecasts made with our model show that smoothing improves the quality of the forecasts.

3. A SEMI-IMPLICIT TIME-STEPPING SCHEME FOR THE ECMWF GLOBAL GRID POINT MODEL

The European Centre's first operational forecasting model is the primitive equation model described in my first two lectures. It has 18624 grid points on each of its 15 horizontal levels, ($\lambda=\Delta\theta=1.875^{o}$), and it includes parameterizations of all the atmospheric physical processes that are thought to be important for forecasting the weather up to ten days ahead (see Tiedtke et al. (1979) for a description of the ECMWF physical parameterization scheme). It is well known that integrations with explicit time-stepping algorithms, such as the leap-frog scheme, requires the use of very small time-steps; the size of the time-step being determined by the highest frequency external gravity wave modes of the model. Over the last ten years we have seen the emergence of two particularly successful optimising techniques, namely (a) semi-implicit methods - Robert et al.(1972), Burridge (1975), Hoskins and Simmons (1975) and Gauntlett and Leslie (1976); and (b) economical explicit schemes based on the method of fractional time-steps - Gadd (1978) and, to some extent, Burridge (1975). In both these methods the approach is to design an efficient algorithm to handle the terms in the model's equations that govern the motion of small amplitude gravity waves. The semi-implicit algorithms, in general, use the undamped Crank-Nicholson scheme with large time-steps, whereas the economic methods, as designed by Gadd (1978) use a sequence of short time-steps for the gravity wave terms. The implicit methods have been criticised because when used with large time-steps the numerical errors incurred may not allow accurate simulation of the process of geostrophic adjustment, Janic and Wiin-Nielsen (1978). This has not been borne out in practice, see Robert et al. (1972) and Burridge (1975).

The efficiency and implementation of semi-implicit algorithms can be best appreciated by considering the following model

problem:-

$$\frac{\partial x}{\partial t} = i\omega x \quad , \text{ with } \omega = \omega_E + \omega_{SI} \tag{3.1}$$

$\omega_E = \omega_E(x)$ and ω_{SI} independent of x and t.

The algorithm

$$\frac{x(t+\Delta t)-x(t-\Delta t)}{\lambda\Delta t} = i\omega_E x(t)+i\frac{\omega_{SI}}{2}(x(t+\Delta t)+x(t-\Delta t)) \tag{3.2}$$

is a typical semi-implicit approximation to (3.1).

If ω_E is constant then (2) is stable provided

$$(\omega_E^m \Delta t)^2 \leq 1 + (\omega_{SI}\Delta t)^2 \tag{3.3}$$

ω_E^m = maximum (ω_E).

If ω_{SI} (>> ω_E) is large, corresponding to the frequency of the external gravity wave modes, then (3.2) is, to all intents and purposes, an unconditionally stable algorithm. For three-dimensional primitive equation models ω_E and ω_{SI} are matrices and the solution of (3.3) requires the inversion of ω_{SI}. For the scheme described in section (3.1) below, this amounts to solving a coupled set of Helmholtz equations on a sphere. The simple stability analysis that results in the criterion (3.3) does not give an accurate indication of the performance of the algorithm for baroclinic models (see Simmons et al. (1978) for a discussion of this point).

Although semi-implicit schemes are currently being used for operational weather forecasting in many national weather services, there have been very few publications of quantitive comparisons between explicit and semi-implicit integrations. In particular, Janic and Wiin-Nielsen's criticisms have

not received any answer. In this lecture I shall describe the semi-implicit scheme that has been designed for the centre's global grid point model, section (3.1), and present results of a case study, section (3.2), which provide at least a partial reply to Janic and Wiin-Nielsen's criticisms.

3.1 The semi-implicit algorithm

The differencing scheme

The complete spatial differencing scheme and the three-dimensional grid was introduced in lecture 2. For the purposes of this lecture we shall consider the following abbreviated set of equations:-

$$\frac{\partial p_s}{\partial t} + \frac{1}{a\cos(\theta)} \{ \delta_\lambda U + \delta_\theta (V\cos(\theta)) \} + \frac{\Delta_\sigma p_s \dot{\sigma}}{\Delta_\sigma \sigma} = 0 \qquad (3.4)$$

$$\frac{\partial u}{\partial t} + \frac{1}{a\cos(\theta)} \{ \delta_\lambda \bar{\phi}^\sigma + R\bar{T}^\lambda \delta_\lambda (\ell n p_s) \} = a_u \qquad (3.5)$$

$$\frac{\partial v}{\partial t} + \frac{1}{a} \{ \delta_\theta \bar{\phi}^\sigma + R\bar{T}^\theta \delta_\theta (\ell n p_s) \} = a_v \qquad (3.6)$$

$$\frac{\partial T}{\partial t} + \frac{1}{p_s} \left\{ \frac{\overline{p_s \dot{\sigma} \Delta_\sigma T}^{\sigma}}{\Delta_\sigma \sigma} - \frac{KT}{\sigma} \overline{(p_s \dot{\sigma} + \sigma \frac{\partial p_s}{\partial t})}^{\sigma} \right\} = a_T \qquad (3.7)$$

for a dry adiabatic version of the model.
The terms a_u, a_v and a_T contain the remaining terms.

We shall need the upper and lower boundary conditions for a K level model

$$(p_s \dot{\sigma})_{\frac{1}{2}} = 0 \qquad (3.8)$$

$$(p_s \dot{\sigma})_{K+\frac{1}{2}} = 0 \qquad (3.9)$$

and the finite difference hydrostatic equation in the form

$$\frac{\Delta_\sigma \phi}{\Delta_\sigma(\ell n \sigma)} = - RT \qquad (3.10)$$

The special treatment required for the polar boundary conditions will only complicate our discussions and so for this lecture we shall disregard this part of the model.

Our semi-implicit scheme follows that of Robert et al. (1972) and is based on a centred scheme in which the linear terms that are responsible for describing the evolution of gravity waves are treated implicitly. For the semi-implicit version we have

$$\partial_t(\overline{\ell n p_s}^t) + \frac{1}{p_s}\frac{1}{a\cos(\theta)}\{\overline{u\delta_\lambda p_s}^\lambda + \overline{v\cos(\theta)\delta_\theta p_s}^\theta\} + \frac{\Delta_\sigma \dot{\sigma}^{2t}}{\Delta_\sigma \sigma} + \frac{1}{a\cos(\theta)}\{\delta_\lambda \bar{u}^{2t} + \delta_\theta(\bar{v}^{2t}\cos(\theta))\} = 0 \qquad (3.11)$$

$$\delta_t \bar{u}^t + \frac{1}{a\cos(\theta)}\{\delta_\lambda \overline{\phi}^{\sigma 2t} + RT_o\delta_\lambda \overline{\ell n p_s}^{2t}\} + \frac{R(\bar{T}^\lambda - T_o)}{a\cos(\theta)}\delta_\lambda(\ell n p_s) = a_u \qquad (3.12)$$

$$\delta_t \bar{v}^t + \frac{1}{a}\{\delta_\theta \overline{\phi}^{\sigma 2t} + RT_o\delta_\theta(\overline{\ell n p_s}^{2t})\} + \frac{R(\bar{T}^\theta - T_o)}{a}\delta_\theta(\ell n p_s) = a_v \qquad (3.13)$$

$$\delta_t \bar{T}^t + \left\{ \frac{\bar{\sigma}^{2t} \Delta_\sigma T_o}{\Delta_\sigma \sigma} - \frac{K T_o}{\sigma} \left(\overline{\bar{\sigma}^{2t} + \sigma \delta_t (\overline{\ell n p_s})^t}^{\sigma} \right) \right\}$$

$$+ \left\{ \frac{\overline{\dot{\sigma} \Delta_\sigma (T - T_o)}^{\sigma}}{\Delta_\sigma \sigma} - \frac{K(T - T_o)}{\sigma} \left(\dot{\sigma} + \sigma \left[\overline{\delta_t \overline{\ell n p_s}^t} \right]_{ex} \right) \right\} = a_T \tag{3.14}$$

where

$$\left[\delta_t \overline{\ell n p_s}^t \right]_{ex} + \frac{1}{p_s} \frac{1}{a \cos(\theta)} \delta_\lambda U + \delta_\theta (V \cos(\theta)) + \frac{\Delta_\sigma \dot{\sigma}}{\Delta_\sigma \sigma} = 0 \tag{3.15}$$

and $\bar{u}^{2t} = \frac{1}{2}(u(t+\Delta t) + u(t-\Delta t))$, etc. (3.16)

Equation (3.15) is used to compute $\dot{\sigma}$ for the terms that are treated explicitly and

$$\left[\delta_t \overline{\ell n p_s}^t \right]_{ex}$$

The temperature $T_o = T_o(\sigma)$ is a standard profile.

In the absence of time truncation, equations (3.11) to (3.14) have the same conservation properties as those of the set (3.4) to (3.7); this may be easily demonstrated using the finite difference rule

$$\delta_\lambda (\bar{A}^\lambda B) = \overline{B \delta_\lambda A}^\lambda + A \delta_\lambda B \tag{3.17}$$

If we introduce the operator Δ_{tt}, defined as

$$\left. \begin{aligned} \Delta_{tt} \psi &= \{\psi(t+\Delta t) + \psi(t-\Delta t) - 2\psi(t)\} \\ &= 2(\bar{\psi}^{2t} - \psi) \end{aligned} \right\} \tag{3.18}$$

and define $\left[\delta_t \overline{\ell n p_s}^t \right]_{SI}$ by

$$\delta_t \overline{\ell np_s}^t = \left[\delta_t \overline{np_s}^t\right]_{ex} + \left[\delta_t \overline{\ell np_s}^t\right]_{SI} \tag{3.19}$$

equations (3.11) to (3.14) may be rewritten in the forms

$$\left[\delta_t(\overline{\ell np_s}^t)\right]_{ex} + \frac{1}{p_s}\frac{1}{a\cos(\theta)}\{\delta_\lambda U + \delta_\theta(V\cos(\theta))\} + \frac{\Delta_\sigma \dot{\sigma}}{\Delta_\sigma \sigma} = 0 \tag{3.20}$$

$$\left[\delta_t \overline{\ell np_s}^t\right]_{SI} + \frac{1}{a\cos(\theta)}\{\delta_\lambda(\tfrac{1}{2}\Delta_{tt}u) + \delta_\theta(\tfrac{1}{2}\Delta_{tt}v\cos(\theta))\} + \frac{\Delta_\sigma(\tfrac{1}{2}\Delta_{tt}\dot{\sigma})}{\Delta_\sigma \sigma} = 0 \tag{3.21}$$

$$\delta_t \ell np_s{}^t - \left[\delta_t \overline{\ell np_s}^t\right]_{SI} = \left[\delta_t \overline{\ell np_s}^t\right]_{ex} = Ap_s \tag{3.22}$$

$$\delta_t \bar{u}^t + \frac{1}{a\cos(\theta)}\left\{\delta_\lambda(\tfrac{1}{2}\Delta_{tt}\bar{\phi}^\sigma) + RT_o\delta_\lambda(\tfrac{1}{2}\Delta_{tt}\ell np_s)\right\} = A_u \tag{3.23}$$

$$\delta_t \bar{v}^t + \frac{1}{a}\left\{\delta_\theta(\tfrac{1}{2}\Delta_{tt}\bar{\phi}^\sigma) + RT_o\delta_\theta(\tfrac{1}{2}\Delta_{tt}\ell np_s)\right\} = A_v \tag{3.24}$$

and

$$\delta_t T^{-t} + \left\{\frac{\overline{\tfrac{1}{2}\Delta_{tt}\dot{\sigma}\Delta_\sigma T_o}^\sigma}{\Delta_\sigma \sigma} - \frac{KT_o}{\sigma}\left(\tfrac{1}{2}\Delta_{tt}\dot{\sigma} + \sigma\left[\delta_t \overline{\ell np_s}^t\right]_{SI}\right)\right\} = T_T \tag{3.25}$$

where Ap_s, A_u, A_v and A_T include all the terms that are computed explicitly.

The stability criterion for this scheme depends on the maximum horizontal wind speed, u/max, and the shortest grid length, Δs_{min}, and takes the form

$$\Delta t_{max} < \frac{\Delta s_{min}}{/u/_{max}} \tag{3.26}$$

This criterion is quite restrictive because of the convergence of the meridians to the poles, and it is necessary to incorporate the spatial filter described in lecture 1. For our operational system this is implemented by filtering the tendencies of the dependent variables $\ell n p_s$, u, v and T. The interaction of the filter and the semi-implicit algorithm is discussed in the next sub-section.

The solution of the semi-implicit system

We first introduce a vector notation in which we define K component vectors by

$$\underset{\sim}{u} = \begin{pmatrix} u_1 \\ u_2 \\ \cdot \\ \cdot \\ \cdot \\ \cdot \\ u_{K-1} \\ u_K \end{pmatrix} \quad \text{etc.} \tag{3.27}$$

where the u_ℓ ($= 1,\ldots,K$) are the u-velocities for levels ℓ. In addition we define ~new variables P by

$$P = \bar{\phi}^{\sigma} + RT_o(\ell n p_s) \tag{3.28}$$

The momentum equations become

$$\delta_t \bar{u}^t + \frac{\mathscr{F}}{a\cos(\theta)} \delta_\lambda(\tfrac{1}{2}\Delta_{tt}\underset{\sim}{P}) = \mathscr{F}\underset{\sim}{A}_u \tag{3.29}$$

$$\delta\underset{\sim}{\bar{v}}^t + \frac{}{a} \delta_\theta(\tfrac{1}{2}\Delta_{tt}\underset{\sim}{P}) = \mathscr{F}\underset{\sim}{A}_v \tag{3.30}$$

where $\mathscr{F} = \mathscr{F}(\theta)$ is the Fourier filtering operator described in my first lecture.

By summation (vertical integration) of the thermodynamic

and continuity equations and use of the hydrostatic equation it can be shown that P satisfies the equation

$$\delta_t \bar{P}^t + \mathcal{F} \underline{\underline{G}} \left(\tfrac{1}{2}\Delta_{tt} \underset{\sim}{d}\right) = \mathcal{F} \underline{A}_p \tag{3.31}$$

where $$\underline{d} = \frac{1}{a\cos(\theta)} \{\delta_\lambda \underset{\sim}{u} + \delta_\theta (\underline{v}\cos(\theta))\} \tag{3.32}$$

and $\underline{\underline{G}}$ is a (K)x(K) matrix.

$\underline{\underline{G}}$ is a function of the standard temperature profile $T_o(\sigma)$. We now define

$$\hat{\underset{\sim}{P}}(t+\Delta t) - \underset{\sim}{P}(t-\Delta t) + 2\Delta t \mathcal{F} A_p(t) \tag{3.33}$$

then we have

$$\underline{P}(t+ t) - \hat{\underset{\sim}{P}}(t+\Delta t) + 2\Delta t \underline{\underline{G}}\, \mathcal{F}\left(\tfrac{1}{2}\Delta_{tt} \underset{\sim}{d}\right) = 0 \tag{3.34}$$

Also we rewrite (3.29) and (3.30) as

$$\underset{\sim}{u}(t+\Delta t) - \hat{\underset{\sim}{u}}(t+\Delta t) + \frac{\Delta t}{a\cos(\theta)} \mathcal{F}\delta_\lambda (\underset{\sim}{P}(t+\Delta t) - \hat{\underset{\sim}{P}}(t-\Delta t)) = 0 \tag{3.35}$$

and

$$\underset{\sim}{v}(t+\Delta t) - \hat{\underset{\sim}{v}}(t+\Delta t) + \frac{\Delta t}{a} \mathcal{F}\delta_\theta (\underline{P}(t+\Delta 4) - \hat{\underline{P}}(t-\Delta t) = 0 \tag{3.36}$$

where

$$\hat{u}(t+\Delta t) = \underset{\sim}{u}(t-\Delta t) + 2\Delta t\, \mathcal{F} \underset{\sim}{A}_u(t) - \frac{\Delta t}{a\cos(\theta)} \mathcal{F}\delta_\lambda (\hat{\underset{\sim}{P}}(t+\Delta t) + \underset{\sim}{P}(t-\Delta t) - 2\underset{\sim}{P}(t) \tag{3.37}$$

$$\hat{\underline{v}}(t+\Delta t) = \underline{v}(t-\Delta t) + 2\Delta t \mathcal{F} \underline{A}_v(t) - \frac{\Delta t}{a} \mathcal{F}\delta_\lambda (\hat{\underset{\sim}{P}}(t+\Delta t) + \underset{\sim}{P}(t-\Delta t) - 2\underset{\sim}{P}(t) \tag{3.38}$$

The divergence of (3.35) and (3.36) gives

$$\underset{\sim}{d}(t+\Delta t)-\hat{\underset{\sim}{d}}(t+\Delta t)+\Delta t\ \frac{1}{a\cos(\theta)}\delta_\lambda \frac{\mathscr{F}}{a\cos(\theta)}\delta_\lambda(P(t+\Delta t)-\hat{\underset{\sim}{P}}(t+\Delta t))$$

$$+\frac{1}{a\cos(\theta)}\delta_\theta(\cos(\theta)\ \frac{\mathscr{F}}{a}\delta_\theta(\underset{\sim}{P}(t+\Delta t)-\hat{\underset{\sim}{P}}(t+\Delta t))$$

$$=0 \qquad (3.39)$$

The elimination of $(\underset{\sim}{P}(t+\Delta t)-\hat{\underset{\sim}{P}}(t+\Delta t))$ between (3.34) and (3.39) gives

$$\underset{\sim}{d}(t+\Delta t)-\underset{\sim}{d}(t+\Delta t)-\Delta t^2\underline{\underline{G}}\delta_\lambda\frac{1}{a\cos(\theta)}\delta_\lambda(\frac{\mathscr{F}}{a\cos(\theta)}\delta_\lambda(\mathscr{F}\Delta_{tt}\underset{\sim}{d}$$

$$+\frac{1}{a\cos(\theta)}\delta_\theta(\cos(\theta)\ \frac{\mathscr{F}}{a}\delta_\theta(\mathscr{F}\Delta_{tt}\underset{\sim}{d}))\qquad =0 \qquad (3.40)$$

a set of coupled finite difference "partial differential equations" for the divergence vector $\underset{\sim}{d}$. Since we need only compute $(\mathscr{F}\Delta_{tt}\underset{\sim}{d})$ we may rewrite (3.40) as

$$(\mathscr{F}\Delta_{tt}\underset{\sim}{d})-\ t^2\underline{\underline{G}}\ \mathscr{F}\left\{(\frac{1}{a\cos(\theta)}\delta_\lambda\ \frac{\mathscr{F}}{a\cos(\theta)}\delta_\lambda(\mathscr{F}\Delta_{tt}\underset{\sim}{d})\right.$$

$$\left.+\frac{1}{a\cos(\theta)}\delta_\lambda(\cos(\theta)\ \frac{\mathscr{F}}{a}\ (\Delta_{tt}d))\right\}$$

$$=\mathscr{F}(\hat{d}(t+\Delta t)+d(t-\Delta t)-2d(t)) \qquad (3.41)$$

The K eigenvalues of the matrix $\underline{\underline{G}}$ are the squares of the phase speeds, C_k^2 $(k=1,---,k)$ of the model's gravity waves in a resting atmosphere with the vertical temperature structure $T_o(\sigma)$. The corresponding eigenfunctions, $Q_k(k=1,\ldots,K)$, of $\underline{\underline{G}}$ describe the vertical structure of these gravity waves. The system of equations (3.41) may be diagonalized or uncoupled using the matrix

$$\underline{\underline{E}} = (\underline{\psi}_1,\ldots,\underline{\psi}_K) \qquad (3.42)$$

where columns are the eigenfunctions of $\underline{\underline{G}}$. This diagonalization is achieved by defining the vector $\underline{Y}$ by the linear transformation

$$\underline{Y} = \underline{\underline{E}}^{-1}(\mathscr{F}\Delta_{tt}\underline{d}) \tag{3.43}$$

and using the well known result $\underline{\underline{E}}^{-1}\underline{\underline{G}}\underline{\underline{E}} = \mathrm{diag}(C_k^2)$ to give

$$Y_k - \Delta t^2 C_k^2 \quad \frac{1}{a\cos(\theta)}\delta_\lambda\left(\frac{\mathscr{F}}{a\cos(\theta)}\delta_\lambda(Y_k)\right)$$

$$+ \frac{1}{a\cos(\theta)}\delta_\theta\left(\cos(\theta)\,\frac{\mathscr{F}}{a}\delta_\theta(Y_k)\right) \quad = f_k \tag{3.44}$$

$$k = 1,\ldots,k$$

for the indivual components of $\underline{Y}$, where

$$\underline{f} = E^{-1}(\hat{\underline{d}}(t+\Delta t) + \underline{d}(t-\Delta t) - 2\underline{d}(t))$$

Polar boundary conditions are required for (3.44) and these may be derived from the special forms of the finite difference equations near the poles. These boundary conditions can be put in the form

$$Y_k(\pm\tfrac{\pi}{2}) - t\,C_k \quad \frac{1}{\frac{a}{2}\cos(\pm\frac{\pi}{2}\mp\frac{\Delta\theta}{2})}\,\frac{1}{a\frac{\Delta\theta}{2}}\,\cos(\pm\tfrac{\pi}{2}\mp\tfrac{\Delta\theta}{2})(Y_k(\pm\tfrac{\pi}{2}) - Y_k(\pm\tfrac{\pi}{2}\mp\Delta\theta)$$

$$= f_k(\pm\tfrac{\pi}{2}) \tag{3.45}$$

where the $\bar{Y}_k(\pm\frac{\pi}{2}\mp\Delta\theta)$ are the zonal means of Y_k on the latitudes $\pm\frac{\pi}{2}\mp\Delta\theta$. Equation (3.45) is a Neumann boundary condition for the zonal means of Y_k, zonal wavenumber zero; all other zonal wavenumbers are zero at the poles. With these polar boundary conditions, (3.44) is solved for $Y_k(k=1,\ldots,k)$ using a direct method involving Fourier analysis in the longitudinal direction and Gaussian elimination in the meridional direction. We can recover $(\mathscr{F}\Delta_{tt}\underline{d})$

from

$$(\mathcal{F}\Delta_{tt}\underset{\sim}{d}) = \underline{\underline{E}}\ \underline{Y} \tag{3.46}$$

Having determined $(\mathcal{F}\Delta_{tt}\underset{\sim}{d})$ we may compute $\ell np_s\ (t+\Delta t)$ and $T(t+\Delta t)$, from the filtered forms of equations (3.22), (3.23) and (3.25). This in turn gives $\underline{P}(t+\Delta t)$ from which $u(t+\Delta t)$ and $v(t+\Delta t)$ can be computed (equations (3.35) and (3.36)).

3.2 Comparative semi-implicit and explicit forecasts

The models and the initial data sets

In this section we shall consider the results of two sets of global ten day forecasts using an explicit version of the ECMWF model and the semi-implicit version described in section 1 above. The resolution of both models is defined by:

$$\Delta\lambda = \frac{360}{64} = 5.625^{o}$$

$$\Delta\theta = \frac{180}{48} = 3.75^{o}$$

9 unequally spaced levels with

$\sigma_k = S_k^2(3-2S_k)$ for $k=\frac{1}{2},1,1\frac{1}{2},\ldots 9,9\frac{1}{2}$.

$S_k = (k-\frac{1}{2})/9$

The physical parameterization used was developed at the Geophysical Fluid Dynamics Laboratory (GFDL); the "1965" version of their parameterization package. The spatial filter used is defined by

$$\Lambda_k = 1 \text{ for } \frac{\cos(\pi/4)}{\cos(\theta)} \sin\left(\frac{k\Delta\lambda}{2}\right) \leq 1$$

$$= 0 \text{ for } \frac{\cos(\pi/4)}{\cos(\theta)} \sin\left(\frac{k\Delta\lambda}{2}\right) > 1\ ,$$

that is, total tendency chopping. The explicit model used the leap-frog time-stepping scheme with a time-step of five minutes, whereas the semi-implicit model used a

time-step of 30 minutes. Both models used a weak time filter to suppress temporal computational modes. In the early stages of the development of the semi-implicit scheme the reference temperature profile $T_o(\sigma)$ was chosen to be the horizontal mean of the initial data and this frequently led to instability.

The instability usually occurred in polar regions with the maximum amplitudes near the tropopause (dry convective adjustment is included in the parameterization scheme which precludes the possibility of static instability being a contributing factor). The reasons for the instability are now understood and have been described by Simmons et al. (1978). For the semi-implicit integrations presented here $T_o = 300^oK$.

The initial data was derived from a GFDL global data set for 1 March 1965. Two data sets were constructed. The first, the uninitialized data, was obtained by bi-linear interpolation from their modified Kurihara grid. The second set, the initialized data, was produced by "balancing" the uninitialized data using the normal mode initialization scheme developed by Temperton and Williamson (1978). The uninitialized data is illustrated by 1000mb and 500mb contour maps in figure (3.1).

The results

Each model was integrated for 10 days from both initial data sets. We shall first deal with the forecasts from the uninitialized data. The five day forecasts of the 1000mb and 500mb northern hemisphere are illustrated in figures (3.2) and (3.3). A synoptic comparison of both forecasts up to five days shows that both models give very similar results with only small differences in amplitude and phase.

In figure (3.4) we have the evolution in time of the

standard deviation and anomoly correlations between the two forecasts for most of the northern hemisphere. In the early part of the forecasts we see that we have quite large differences which reach a maximum at around day one, thereafter the two scores indicate that the models become closer together until about day five. After day five the models again diverge. The large differences between the two models in the first two days presumably arise from some initial imbalance between the mass and wind fields. This conjecture is supported by the results of the forecasts from the initialized data. The forecasts from the initialized are illustrated in figures (3.5), (3.6) (day 5 maps) and (3.7) (standard deviation and correlations). In this second set of forecasts both models agree remarkably well and the differences become significant only after 7 days. As the two objective scores show the semi-implicit and explicit forecasts do eventually differ from each other but, as can be seen from figure (3.8) which shows explicit and semi-implicit ten day forecasts of the 1000mb contour heights, these differences are not significant synoptically.

These results are in accord with Janjić and Wiin-Nielsen's (1978) conclusions. Namely, provided the initial data is well balanced we can expect semi-implicit integrations with large time-steps to be as accurate as explicit integrations.

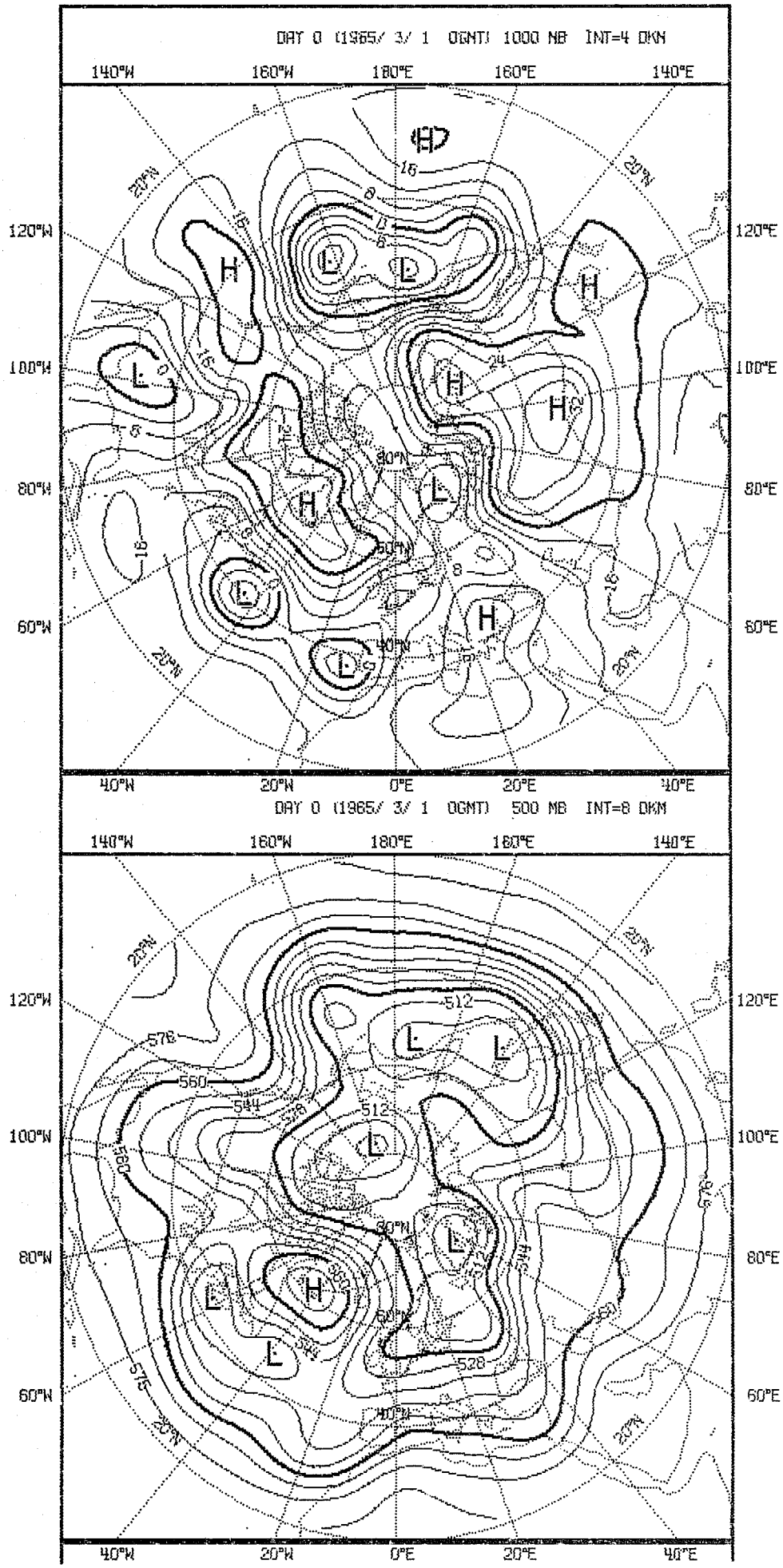

Fig. 3.1 Initial data 1965/3/1 0GMT.

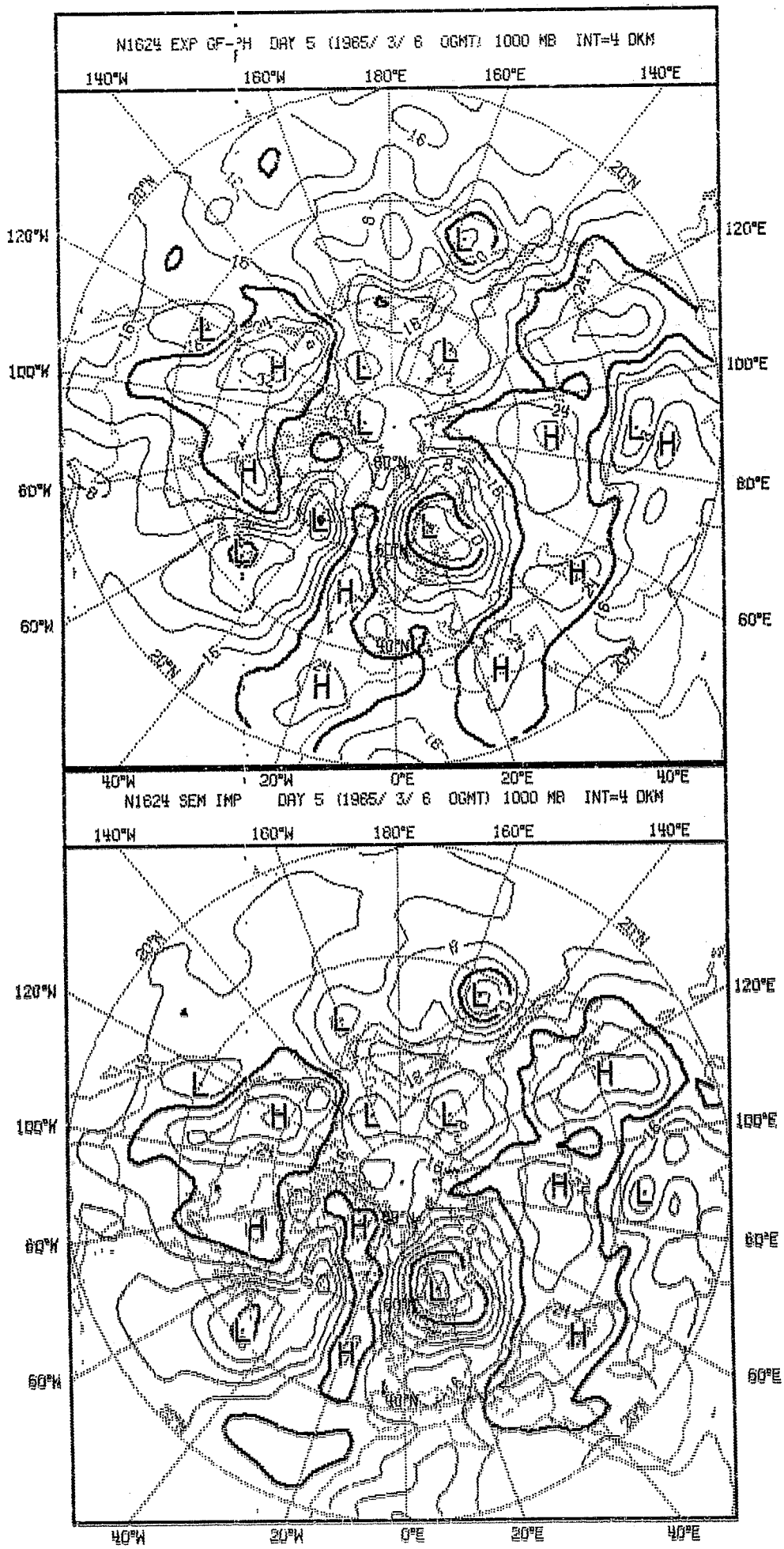

Fig. 3.2 5 day forecast uninitialized data. Explicit integration upper frame, semi-implicit integration lower frame.

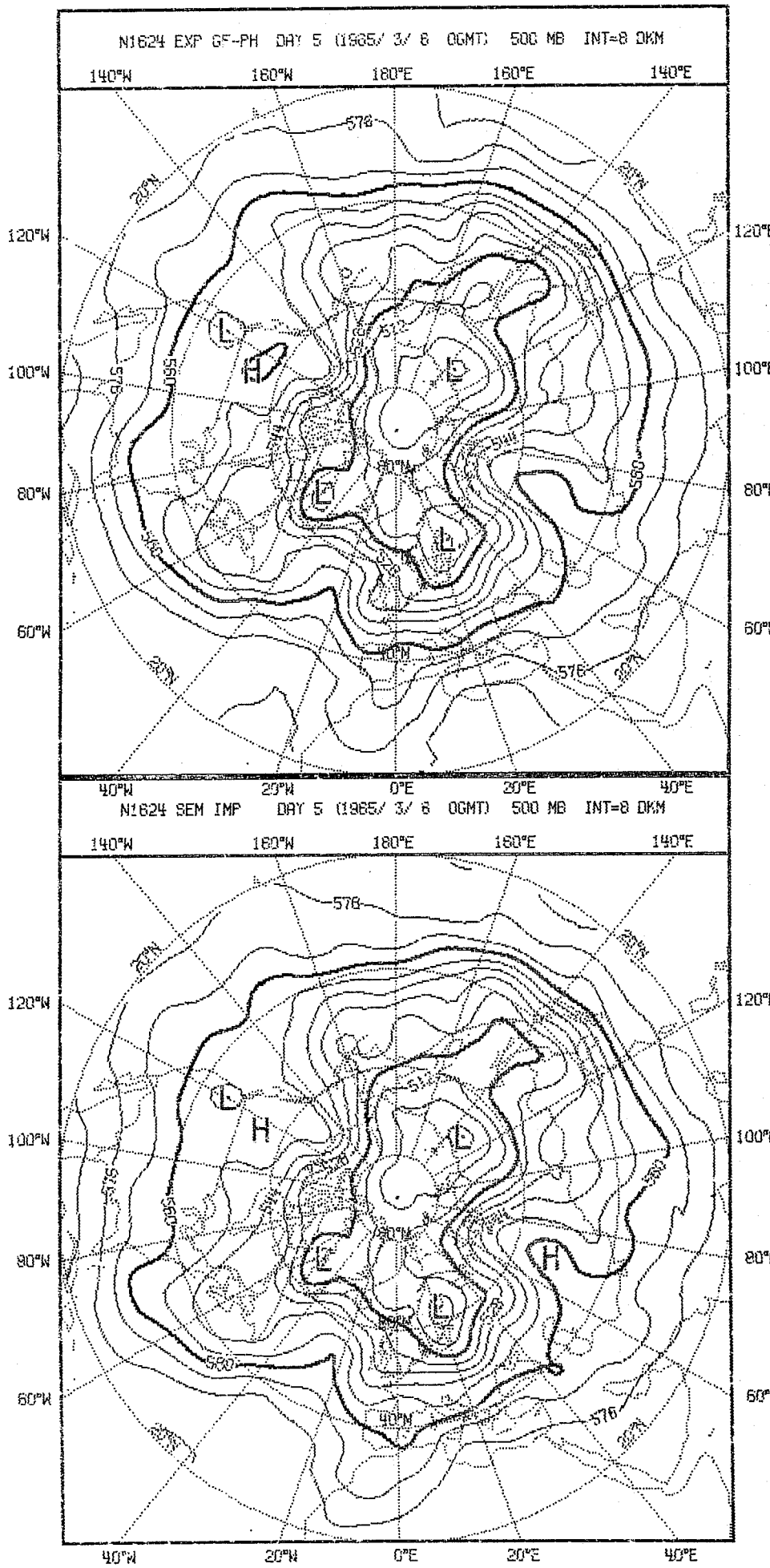

Fig. 3.3 5 day forecast uninitialized data. Explicit integration upper frame, semi-implicit integration lower frame.

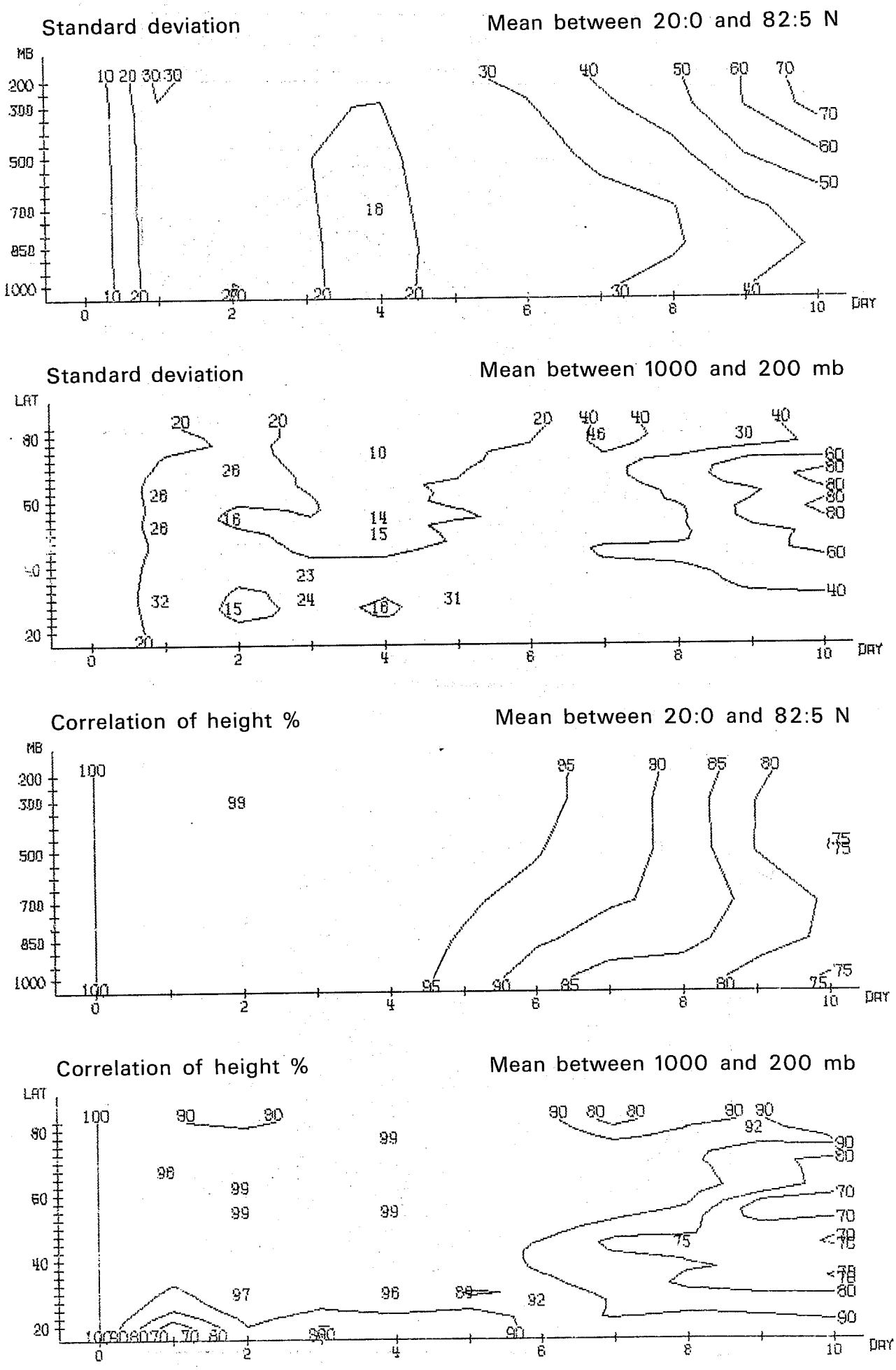

Fig. 3.4 Standard deviations and correlations for the uninitialized integrations.

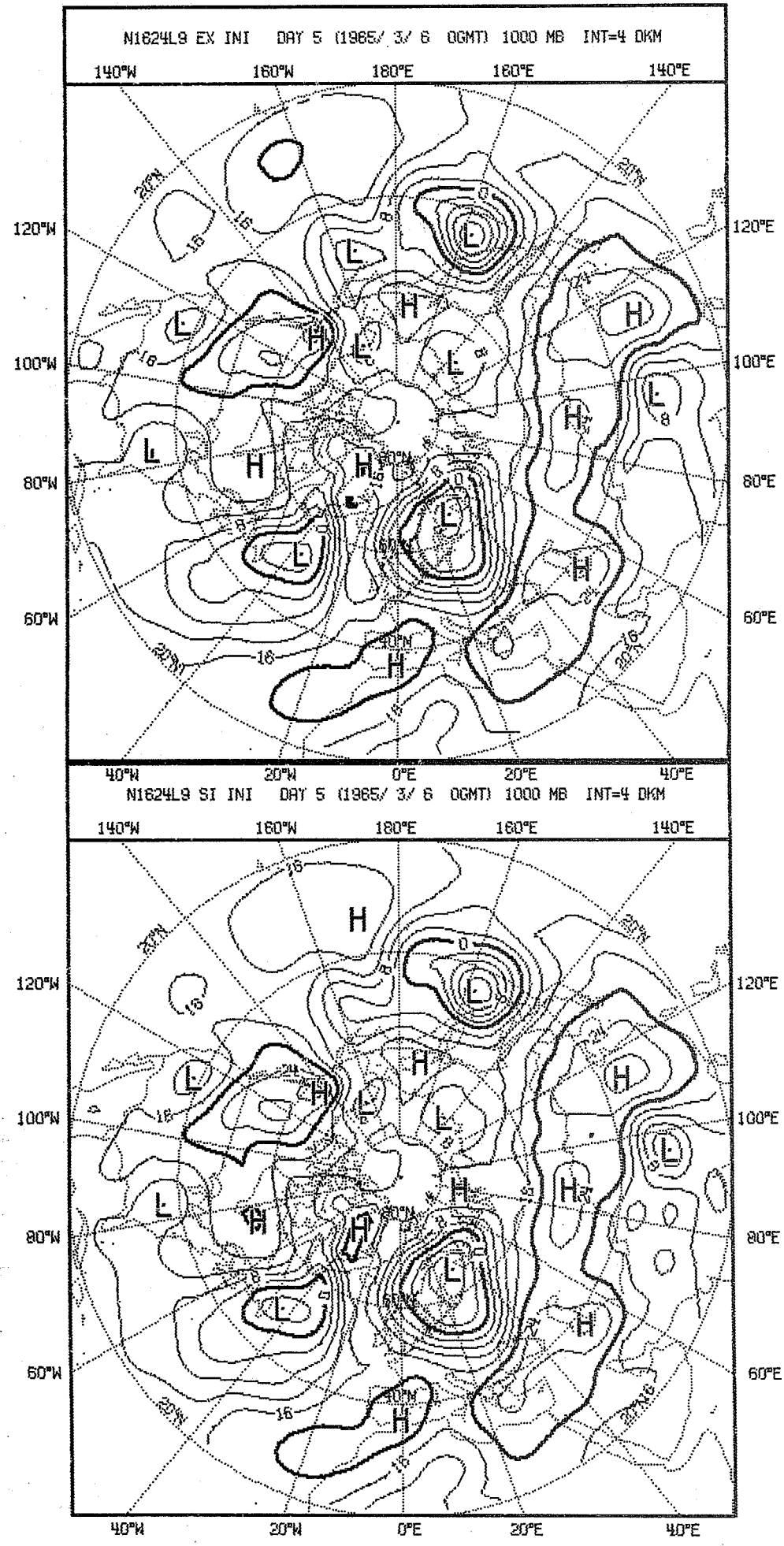

Fig. 3.5 5 day forecast initialized data. Explicit integration upper frame, semi-implicit integration lower frame.

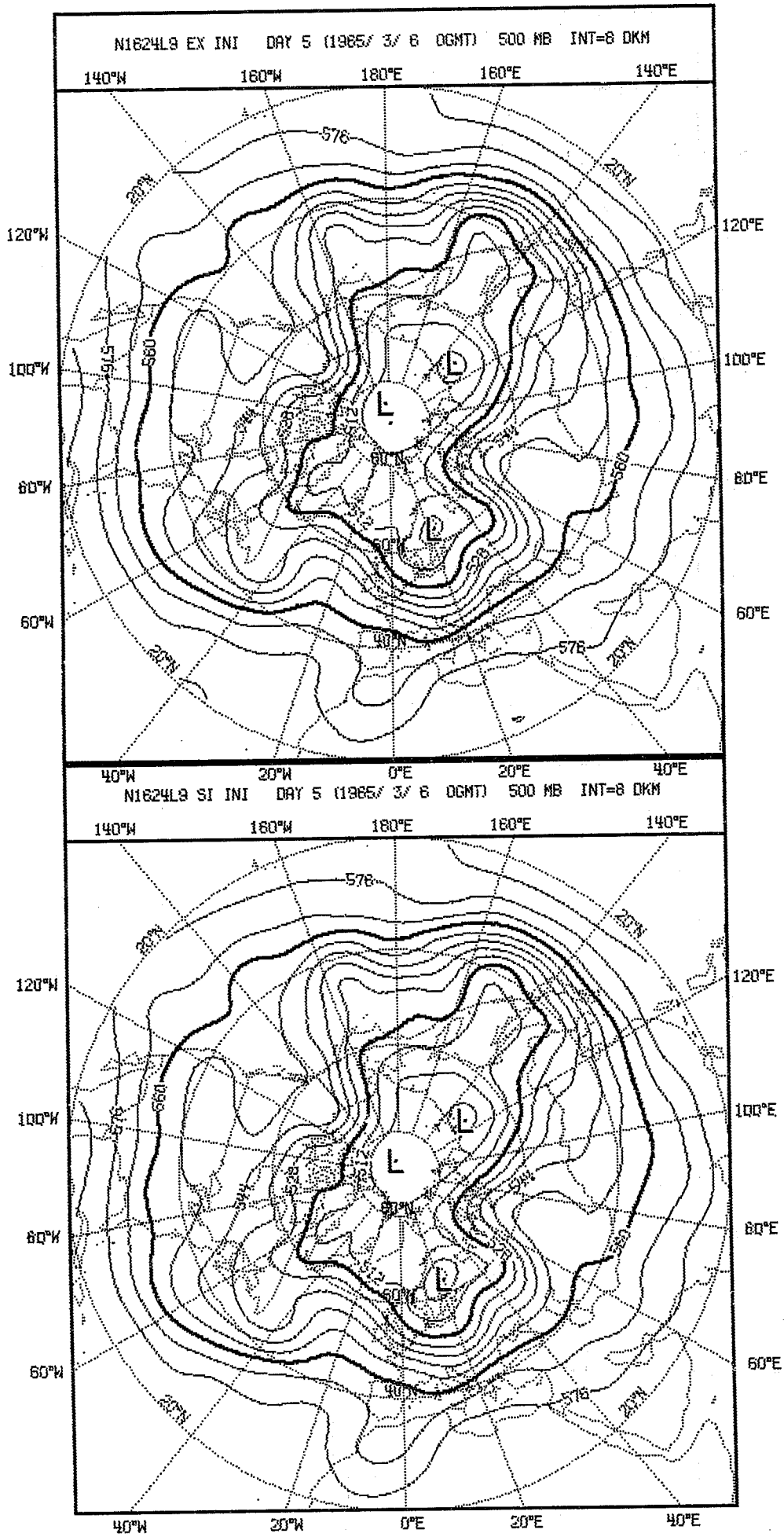

Fig. 3.6 5 day forecast initialized data. Explicit integration upper frame, semi-implicit integration lower frame.

4. LATERAL BOUNDARY CONDITIONS FOR LIMITED AREA MODELS

INTRODUCTION

Most operational forecasting models in use in the national weather services are limited area models, and as such require boundary values and special "boundary schemes" at the lateral boundaries. This is understandable since the cost of integrating global models with adequate resolution (grid lengths between 50 and 200km say) for short range operational forecasting is enormous and prohibitive for most national centres. Numerical studies of small scale phenomena such as convection, fronts, sea breezes are usually carried out with fine mesh (grid lengths between 10 and 20km) limited area grid point models. The boundary conditions for these integrations are usually maintained constant throughout the period of the forecast or are derived from forecasts made with another model which covers a larger area.

In this lecture I shall discuss lateral boundary conditions for simple one dimensional models and give an example of boundary induced instabilities with an otherwise stable finite difference scheme. Some of the problems arising with two and three dimensional primitive equation models are discussed. Finally, some results using a boundary relaxation technique are described. It is obviously impossible within the space of a single lecture to cover the many schemes that have been tried and the interested reader is referred to the comprehensive review paper by Sundström and Elvius (1979).

4.1 The linear advection equation

Firstly, we consider the following initial value problem

$$\frac{\partial \phi}{\partial t} - u \frac{\partial \phi}{\partial x} = 0 \qquad 0 \leq x \leq a, \; t \geq 0, \; u > 0 \qquad (4.1)$$

$$\phi(x,0) = f(x) \tag{4.2}$$

Equation (4.1) and initial conditions (4.2) have the solution

$$\left.\begin{aligned} &\phi(x,t) = f(x+ut) \\ &\text{for} \qquad 0 \leqslant x+ut \leqslant a. \end{aligned}\right\} \tag{4.3}$$

In order to prescribe the solution for times $t > (a-x)/u$ we need boundary conditions for $t > 0$. From physical considerations, the velocity u advects ϕ from right to left, we could choose

$$\phi(a,t) = g(t) \qquad t \geqslant 0 \tag{4.4}$$

and this leads to the solution

$$(x,t) = g\left(t + \frac{x-a}{a}\right) \tag{4.5}$$

for $t > (a-x)/u$.

The solution comprising (4.3) and (4.5) obviously satisfies our initial boundary value problem for (4.1).

In figure (4.1) we can see which parts of the space-time diagram that are influenced by the boundary and initial values. The lines x+ut = constant are called characteristics, along which the solution is constant. As a consequence the solution at the "outflow" boundary, x = 0, is determined by "interior" values. With the boundary condition (4.4) the initial value problem (4.1) and (4.2) is properly posed in the sense of Hadamard, in that the solution depends continuously on the initial and boundary values. Any discontinuities arise from the initial and boundary values only. If the boundary values are prescribed at x=0, the problem is in general "ill-posed".

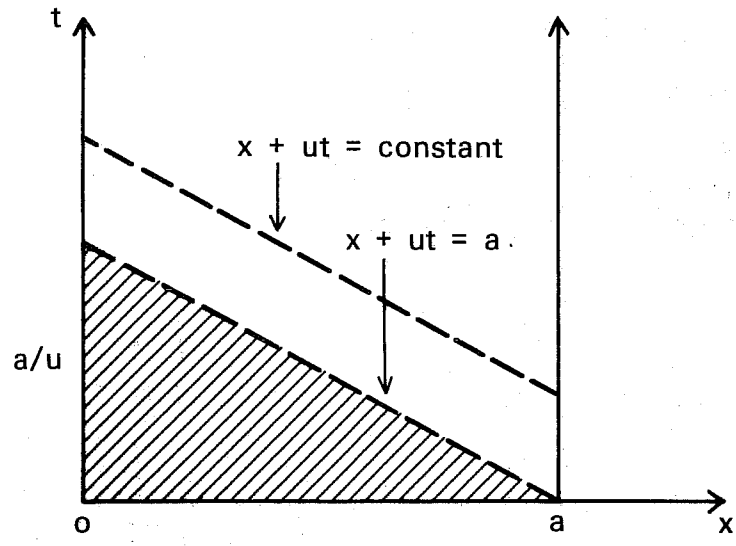

Fig. 4.1 Space/time diagram for equation (4.1).

We now turn to a finite difference approximation for ϕ. Our discussion in the rest of this section is based on Kreiss's (1971) paper. We first consider the right hand quater plane problem

$$\left.\begin{aligned} &\frac{\partial\phi}{\partial t} - \frac{u\partial\phi}{\partial x} = 0, \quad u \geqslant 0 \\ &x \geqslant 0,\ t \geqslant 0 \\ &\phi(x,0) = f(x),\ \int_0^\infty |f(x)|^2 dx < \infty \end{aligned}\right\} \qquad (4.6)$$

The solution of (4.6) is

$$\phi(x,t) = f(x+ut) \qquad (4.7)$$

for all $t \geqslant 0$. Again we note the absence of any condition at $x = 0$. For our finite difference approximation we use the space-time grid defined by

$$x_j = j\Delta x \qquad \Delta x = 1/N \quad (N \text{ integral})$$

$$t_n = n\Delta t \quad ,$$

$$\phi_j^n = \phi(x_j, t_n)$$

The derivatives in (4.1) are approximated by centred differences to give

$$\left.\begin{aligned} &\frac{\phi_j^{n+1} - \phi_j^{n-1}}{2\Delta t} - u\frac{(\phi_{j+1}^{n} - \phi_{j-1}^{n})}{2\Delta x} = 0 \\ &\text{that is } \phi_j^{n+1} = \phi_j^{n-1} + \lambda(\phi_{j+1}^{n} - \phi_{j-1}^{n}),\ \lambda = \frac{u\Delta t}{\Delta x} \\ &\qquad \text{for } j = 1,2,..... \\ &\text{with} \qquad \phi_j^{o} = f(x_j) \end{aligned}\right\} \quad (4.8)$$

For the finite difference solution ϕ_j^n we need to specify ϕ_j^1 and for our analysis we assume

$$\phi_j^1 = g(x_j) \qquad (4.9)$$

For our discussion we shall consider the boundary condition

$$\phi_o^n = \beta\phi_1^n \qquad (4.10)$$

The Ryabenkii-Godunow condition for stability requires that there exists <u>no</u> solutions of the form

$$\phi_j^n = Z^n P_j, \quad P_j \neq 0 \qquad (4.11)$$

with $|Z|>1$ and $\Sigma_j |P_j|^2 \Delta x < \infty$

Note that the space dependence is bounded. If there are solutions of this form, then choosing the bounded initial conditions $\phi_j^o = ZP_j$, $\phi_j^1 = ZP_j$ for the appropriate P_j and Z will result in instability. In addition we shall assume that the Courant Friedrichs Lewy criterion $|\lambda| < 1$ is satisfied.

Substitution of (4.11) into (4.8) gives

$$(Z^2-1)P_j = \lambda Z(P_{j+1} - P_{j-1}) \qquad (4.12)$$

which has solutions of the form

$$P_j = \alpha_1 \kappa_1^j + \alpha_2 \kappa_2^j \tag{4.13}$$

with the κ_i (i=1,2) satisfying the equation

$$(Z^2-1)\,\kappa = \lambda(\kappa^2-1)Z \tag{4.14}$$

Either both roots of (4.14) lie on the unit circle or one ($\kappa=\kappa_1$) root lies inside and the other ($\kappa=\kappa_2$) outside. If $|\lambda| < 1$ and $|Z|$ is large enough, $|Z| > 1$, we have $|\kappa_1| < 1$ and $|\kappa_2| > 1$ with

$$\kappa_1 = \left(\frac{Z^2-1}{2Z}\right)\frac{1}{\lambda} - \sqrt{\left(\frac{Z^2-1}{2Z}\right)^2 \frac{1}{\lambda^2} + 1} \quad < 0, \text{ for } Z > 0$$

$$\kappa_1 = \left(\frac{Z^2-1}{2Z}\right)\frac{1}{\lambda} + \sqrt{\left(\frac{Z^2-1}{2Z}\right)^2 \frac{1}{\lambda^2} + 1} \quad > 0, \text{ for } Z < 0.$$

In order to satisfy $\sum_{j=1}^{\infty} |P_j|^2 \Delta x < \infty$ we select

$$P_j = \alpha_1 \kappa_1^j \qquad |\kappa_1| < 1.$$

The boundary condition (4.10) gives

$$\kappa_1 \beta = 1 \tag{4.15}$$

and therefore if $|\beta| < 1$ we have no amplifying solutions of the form (4.15). For $|Z|$ large we have unstable solutions at least for

$$\beta < -1 \qquad (Z > 0)$$

and $$\beta > \frac{1}{\lambda} + \sqrt{\frac{1}{\lambda^2} + 1} \qquad (Z < 0)$$

Our stability analysis indicates a region of stability, namely $|\beta_1| < 1$, but the initial value problem with

$$\left.\begin{aligned} &\beta = 1 \\ &\phi_j^o = 1 \qquad \text{for } j = 1 \\ &\quad = 0 \qquad \text{for } j > 1 \\ &\phi_j^1 = 0 \qquad \text{all } j \end{aligned}\right\}$$

which is stable according to the Ryabenkii-Godunow criterion has a solution

$$\sum_{j=1}^{\infty} |\phi_j|^2 \Delta x \sim \text{constant } \sqrt{n} = \text{constant } (t/\Delta t)^{\frac{1}{2}} \qquad (4.16)$$

an algebraic growth in time which can easily be controlled by smoothing. This type of solution is not covered by the exponential form Z^n of the Ryabenkii-Godunow conditions. We next show that restricting the "area" of integration to a finite interval leads to exponentially growing solutions for the scheme (4.8), (4.9) and (4.10). We now consider the finite difference solution of

$$\left.\begin{aligned} &\frac{\partial \phi}{\partial t} - u\frac{\partial \phi}{\partial x} = 0 \\ &0 < x < a \\ &\phi(x,0) = f(x) \\ &\phi(0,t) = 0 \end{aligned}\right\} \qquad (4.17)$$

using the centred scheme (4.8) with the boundary conditions

$$\left.\begin{aligned} &\phi_o^n = \phi_1^n (\beta = 1) \\ &\phi(a,t) = 0 \equiv \phi_N^n = 0 \\ &N\Delta x = a \end{aligned}\right\} \qquad (4.18)$$

Again we look for solutions of the form

$$_j^n = Z^n P_j = Z^n(\alpha_1 \kappa_1^j + \alpha_2 \kappa_2^j)$$

The boundary conditions at x = 0 and x = a give

$$\alpha_1\kappa_1 + \alpha_2\kappa_2 = \alpha_1 + \alpha_2$$

$$\alpha_1(\kappa_1-1) + \alpha_2(\kappa_2-1) = 0 \qquad (4.19)$$

(Note $\kappa_1\kappa_2 = -1$)

which for non-trivial solutions for α_i(i=1,2) requires

$$\begin{vmatrix} \kappa_1^{2N} & (-1)^N \\ (\kappa_1-1) & -(1 + \kappa_1^{-1}) \end{vmatrix} = 0$$

that is $(1+\kappa_1)\ (\kappa_1)^{2N-1} = (-1^N\ (1-\kappa_1)$. Restricting N to be even gives

$$(\kappa_1)^{2N-1} = \frac{1-\kappa_1}{1+\kappa_2} \qquad (4.20)$$

For large N (4.20) has a solution for κ_1 very near 1. We look for solutions of the form

$$\kappa_1 = 1- \{\frac{1}{2N}\ \ell n(\mu N + \frac{\nu \ell n(\ell n(N))}{N}\}$$

This gives

$$(\kappa_1)^{2N-1} = \left\{ 1 - \left[\frac{1}{2N}\ \ell n(\mu N) + \frac{\nu \ell n(\ell nN)}{N} \right] \right\}^{2N-1}$$

$$\sim \exp\left\{ -(2N-1)\ (\frac{1}{2N}\ n(\mu N) + \frac{\nu \ell n(\ell n(N))}{N}) \right\}$$

$$\sim \exp\left\{ -\ell n(\mu N) \right\} \left\{ \exp\ -2\nu \ell n(\ell n(N)) \right\}$$

$$= \frac{1}{\mu N}\ \exp\left\{ \{-2\nu \ell n(\ell nN) \right\},$$

and in order to balance the leading terms on the right hand side of (4.20) we require $\mu = 4$ and $\nu = -\frac{1}{2}$ giving the asymptotic result

$$\kappa_1 = 1 - \frac{1}{2N}\,\ell n(N) + O(\ell n\frac{(\ell n(N))}{N}) + O(\frac{1}{N}) \qquad (4.21)$$

for an approximate solution of (4.20) with $(\kappa_1) < 1$.

For $\kappa_1 > 0$ we have $Z < 0$ and for κ_1 given by (4.21) a simple calculation gives

$$Z = -\,(1 + \tfrac{1}{2}\lambda\frac{\ell n(N)}{N}) \ .$$

This gives

$$Z^n = (-1)^n\,(1 + \tfrac{1}{2}\lambda\frac{\ell n(N)}{N})^n$$

$$= (-1)^n\,(1 + \frac{u\Delta t}{2(N\Delta x)}\,\ell n(N)\,)^n$$

$$\sim (-1)^n \exp\{\frac{ut}{2a}\,\ell n(N)\} = (-1)^n\,N^{(ut/2a)} \qquad (4.22)$$

Here our finite difference solution, (4.8) and (4.18), to our initial boundary value problem (4.17) has exponentially growing solutions.

Kreiss (1971) and Gustaffsson (1972) have strengthened the Ryabenkii-Godunow stability criteria to cover the possibility of algebraically growing disturbances for the right hand quarter plane problem (4.6). They impose the constraint that there must be no bounded (in space) solutions for $|Z| > 1$ and for $|Z| = 1 + \varepsilon$, $\varepsilon > 0$, as $\varepsilon \to 0$.

In addition they show that a finite difference solution to (4.17) is stable if $|\lambda| < 1$ and the associated right hand ($x > 0$) and left-hand ($x < a$) quarter plane problems are stable according to their strengthened form of the Ryabenkii-Godunow stability criterion.

Now consider the boundary treatment

$$\phi_0^{n+1} = \frac{1}{\Delta x}\,(u\Delta t\phi_1^n + (\Delta x - u\Delta t)\phi_0^n)$$

that is extrapolation using the fact that the solution is constant along characteristics, $x + ut = \text{constant}$. This can be written as

$$\phi_0^{n+1} = \phi_0^n + \lambda(\phi_1^n - \phi_0^n) \qquad (4.23)$$

Kreiss (1971) has shown that (4.23) is a stable formulation for ϕ_0^{n+1}. Also, Richtmyer & Morton (1967) (page 141) have shown that the extrapolation

$$\phi_1^{n+1} = \tfrac{1}{2}(\phi_1^{n-1} + \phi_1^{n+1}) \qquad (4.24)$$

is stable, in this case ϕ_1^{n+1} is determined from

$$\phi_1^{n+1} = \frac{1}{1+\frac{1}{2}\lambda}\ (1-\tfrac{1}{2}\lambda)\phi_1^{n-1} + \lambda\phi_2^n \qquad (4.25)$$

4.2 Advection and gravity waves

The linearized shallow water wave equations in one dimension can be written as

$$\left.\begin{aligned} &\frac{\partial u'}{\partial t} + U_o\frac{\partial u'}{\partial x} + \frac{\partial \phi'}{\partial x} - fv' = 0 \\ &\frac{\partial v'}{\partial t} + U_o\frac{\partial v'}{\partial x} + fu' = 0 \\ &\frac{\partial \phi'}{\partial t} + U_o\frac{\partial \phi'}{\partial x} - fU_o' + \Phi_o\frac{\partial u'}{\partial x} = 0 \end{aligned}\right\} \qquad (4.26)$$

$$0 < x < a$$

where U_o = constant, $\partial\Phi_o/\partial y + fU_o = 0$

The three equations in (4.26) can be reduced to a single equation for u , namely

$$\left(\frac{\partial}{\partial t} + U_o\frac{\partial}{\partial x}\right)\left\{\left(\frac{\partial}{\partial t} + U_o\frac{\partial}{\partial x}\right)^2 u' - c^2\frac{\partial^2 u'}{\partial x^2} + f^2u'\right\} + f^2U_o\frac{\partial u'}{\partial x} = 0 \qquad (4.27)$$

The boundary conditions for (4.27) depend only on the values of the three characteristic velocities U_o, $U_o+\sqrt{\Phi}$ and $U_o-\sqrt{\Phi}_o$. At x = 0 we need a boundary condition for each positive characteristic velocity; whereas at x = 0 we need a

boundary condition for each negative characteristic velocity. Since the Coriolis terms have no influence on the mathematical problems associated with specification of boundary values we neglect terms in f for the remainder of this section. If we define characteristic variables $\alpha = u' + \phi'/\sqrt{\Phi}_o$, $\beta = u' - \phi'/\sqrt{\Phi}_o$, (4.26) may be rewritten as ($f \equiv 0$)

$$\left.\begin{aligned} &\frac{\partial \alpha}{\partial t} + (U_o + \sqrt{\Phi}_o)\frac{\partial \alpha}{\partial x} = 0 \\ &\frac{\partial v}{\partial t} + U_o\frac{\partial v}{\partial x} = 0 \\ &\frac{\partial \beta}{\partial t} + (U_o - \sqrt{\Phi}_o)\frac{\partial \beta}{\partial x} = 0, \end{aligned}\right\} \qquad (4.28)$$

namely a system of three independent advection equations. Therefore for positive $U_o < \sqrt{\Phi}_o$ we should specify α and v at $x = 0$, and β at $x = a$ in order to have a mathematically well posed problem. In addition for a finite difference treatment of (4.28) we require a stable scheme for β at $x = 0$ and α and v at $x = a$.

4.3 The primitive equations in two and three dimensions

For the primitive equations in two or three dimensions the problems are obviously more difficult to analyse. For the shallow water wave equations in two dimensions Sundström and Elvius (1979) analyse the general problem for boundaries at x = constant. Their approach is to "Fourier analyse out" the y, tangential dependence and use a Laplace transform in time to reduce the system to a coupled set of ordinary differential equations in x to which a diagonalization procedure similar to that described in (2.2) may be applied.

In three dimensions the problem is further complicated by the fact that the primitive equations do not constitute a hyperbolic set of equations. Oliger and Sundström (1978) have suggested an approach based on expanding the vertical dependence in terms of the eigenfunctions of the vertical

differential operators, which for a linearized system can be reduced to sets of uncoupled two-dimensional systems. These two-dimensional systems are then treated individually.

4.4 A boundary relaxation scheme

In this sub-section we shall discuss an alternative to the strictly mathematical approach described in the last three sub-sections. Here we deliberately specify all variables on the boundaries and inhibit the development of any boundary induced instabilities that could arise by including extra terms in the governing equations. Kållberg (1977) has tested such a scheme in a limited area barotropic model. For his model the equations are

$$\left.\begin{aligned} &\frac{\partial u}{\partial t} - (f+\zeta)v + \frac{\partial}{\partial x}(\phi+\tfrac{1}{2}(u^2+v^2)) = -k(u-\tilde{u}) \\ &\frac{\partial v}{\partial t} + (f+\zeta)u + \frac{\partial}{\partial y}(\phi+\tfrac{1}{2}(u^2+v^2)) = -k(v-\tilde{v}) \\ &\frac{\partial \phi}{\partial t} + \frac{\partial}{\partial x}(\phi u) + \frac{\partial}{\partial y}(\phi v) = -k(\phi-\tilde{\phi}) \end{aligned}\right\} \quad (4.29)$$

where k is large in some boundary zone, $\tilde{u}$, $\tilde{v}$ and $\tilde{\phi}$ are externally prescribed fields. The finite difference approximations to the left hand sides in (4.29) are the cartesian equivalent of the scheme used for the centres global grid point model. The time-stepping algorithm for (4.29) is of the form

$$\frac{X(t+\Delta t) - X(t-\Delta t)}{2\Delta t} + F(X(t)) = -k(X(t+\Delta t)-X(t+\Delta t) \quad (4.30)$$

where X is a vector consisting of all the models variables and F represents the spatial dependence on the left hand sides of (4.29). Equation (4.30) can be rewritten as

$$\left.\begin{aligned} \hat{X}(t+\Delta t) &= X(t-\Delta t) - 2\Delta t\, F(X(t)) \quad , \\ X(t+\Delta t) &= (1-\alpha)\hat{X}^{n+1} + \alpha \tilde{X}^{n+1} \quad , \\ \text{and} \quad \alpha &= 2\Delta t - k/(1+2\Delta t k) = 1-\tanh(j/2) \, , \end{aligned}\right\} \qquad (4.31)$$

where j is the number of grid lengths to the nearest boundary. The values of α are given in table 1.

j	α
0	1.000
1	.538
2	.238
3	.095
4	.036
5	.013
6	.005
7	.002
8	0

Table 1 $\alpha = 1 - \tanh(j/2)$

This boundary scheme is a simplified version of a procedure designed by Davies (1976).

In one of Källberg's tests of this scheme, geostrophically balanced waves in a cyclic β-plane ($f=f_o+\beta y$) channel with $\Delta x=\Delta y=300$km were integrated to provide the external boundary forcing ($\tilde{X}$) for an embedded limited area (40x40 grid points) with $\Delta x=\Delta y=100$km. In figure (4.2) the initial fields are shown for the full cyclic area with the limited area delineated by the inner frame. 48-hour forecasts for the limited and coarse mesh areas are illustrated in figure (3). The limited area and coarse

mesh forecasts agree well with each other with no discernible boundary noise. Other tests performed by Källberg also demonstrated that large scale gravity waves were successfully absorbed in the relaxation zone.

4.5 Summary

We have seen that numerical instabilities can arise as the result of using computational boundary conditions with an otherwise stable scheme. No doubt it is best to base formulations for lateral boundary schemes on physical considerations such as the number of outgoing characteristics, but ad hoc techniques such as the relaxation scheme described in (4.4) can provide simple stable schemes possibly at the expense of accuracy. For studies of special phenomena, for example frontogenesis, cumulus convection, etc., this could be by far the most cost effective approach. Whatever method is used the useful period of the limited area forecast depends on how quickly the errors generated at the boundary propagate into the interior and it is particularly important to prevent these errors with large amplitudes from being propagated at the speed of the external gravity waves, about $300 m^{s-1}$. Källberg's use of Davies relaxation technique certainly prevents this from occuring in barotropic models. With more and more research groups coming to rely on limited area models for forecasting and research the special techniques necessary to provide stable accurate computational boundary conditions deserves much more intensive investigation.

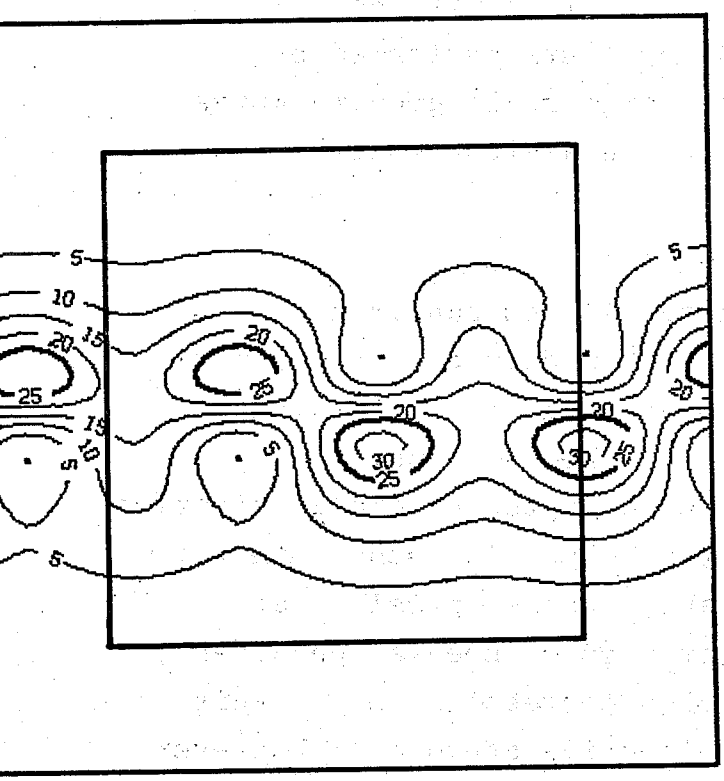

-COMPONENT 0:01

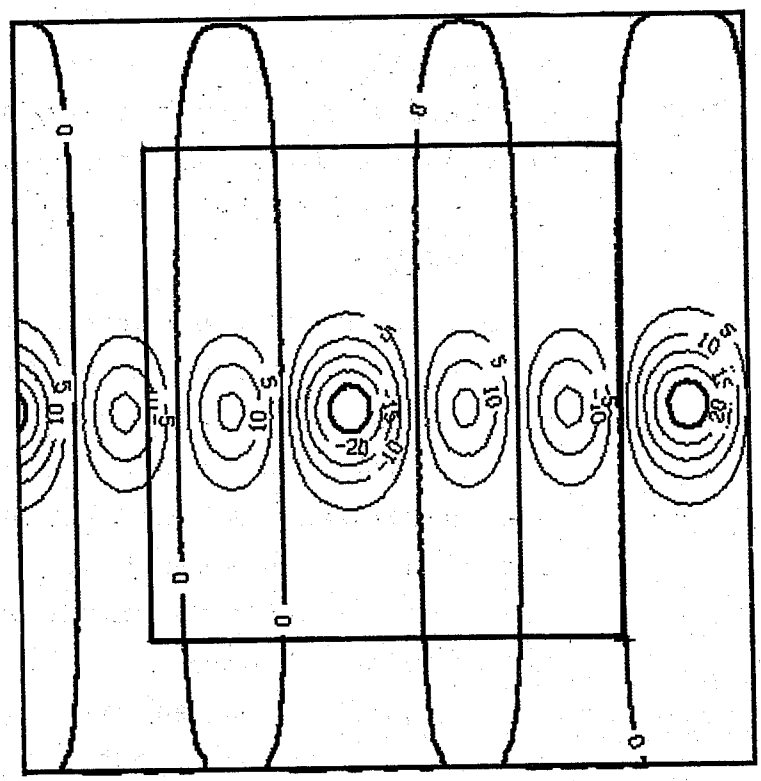

V-COMPONENT 0:01

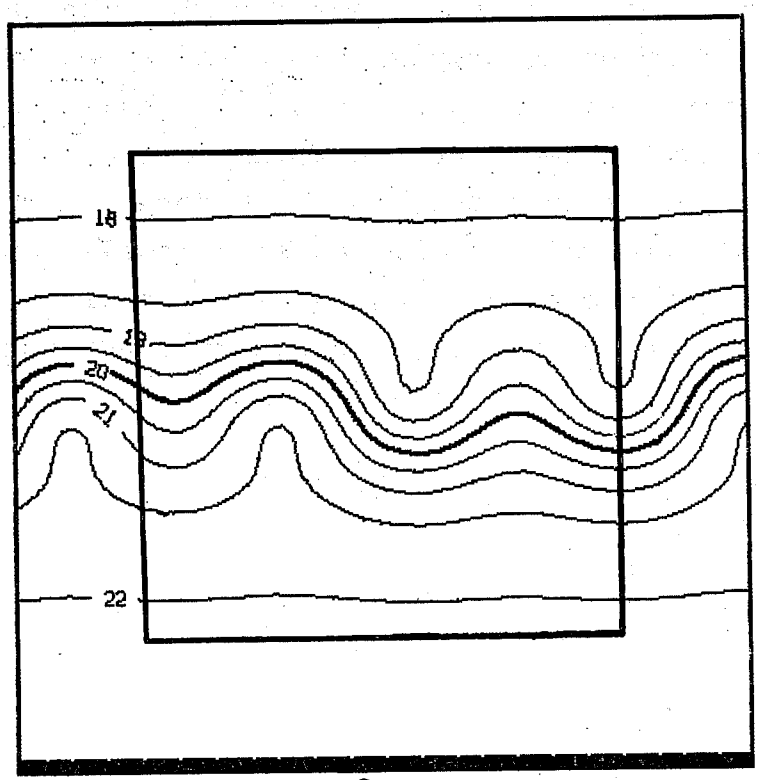

GEOPOTENTIAL × 10^{-3}

Fig. 4.2 Initial fields in the full cyclic area. The limited area is outlined by the inner frame. Winds in $msec^{-1}$. Geopotential in m^2 sec^2.

U-COMPONENT 48 V-COMPONENT 48 GEOPOTENTIAL × 10^{-3}

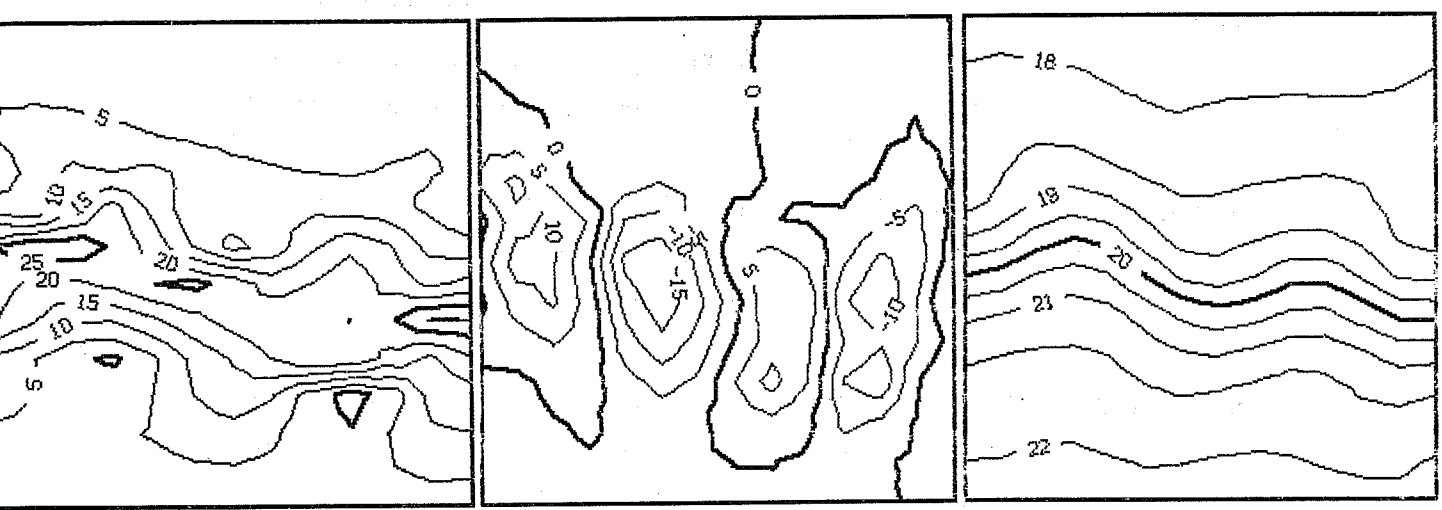

U-COMPONENT 48 V-COMPONENT 48 GEOPOTENTIAL × 10^{-3}

Fig. 4.3 48 hour forecast. Limited area upper frames, coarse mesh lower frames.

References

Arakawa, A., 1966: "Computational design for long term integrations of the equations of fluid motion". J. Comp. Phys., 1, 119-143.

Arakawa, A. & Lamb, V., 1977: "Computational Design of the Basic Dynamical Processes of the UCLA General Circulation Model". Methods in Computational Physics, Vol.17. Edited by J. Chang.

Burridge, D.M., 1975: "A split semi-implicit reformulation of the Bushby-Timpson 10-level model". Quart. J.R. Met. Soc., 101, 777-792.

Burridge, D.M. & Haseler, J., 1977: "A model for medium range weather forecasting". ECMWF Technical Report No. 4.

Chang, J. (Editor), 1977: "Methods in Computational Physics". Volume 17, "General Circulation Models of the Atmosphere". Academic Press.

Davies, H.C., 1976: "A lateral boundary formulation for multi-level prediction models". Quart. J.R. Met. Soc., 102, 405-418.

Gadd, A.J., 1978: "A split explicit integration scheme for numerical weather prediction". Quart. J.R. Met. Soc., 104, 569-582.

Gates, W.L., Batten, E.S., Kahle, A.B. & Nelson, A.B., 1971: "A Documentation of the Mintz-Arakawa two-level Atmospheric General Circulation model", R-877-ARPA Rand Corp.

Gauntlett, D.J., Leslie, L.M. & Hincksman, D.R., 1976: "A semi-implicit forecast model using the flux form of the primitive equations". Quart. J.R. Met. Soc., 102, 203-217.

Gauntlett, D.J., Burridge, D.M. & Arpe, K., 1977: "Comparative Extended Range Numerical Integrations with the ECMWF Global Forecasting model 1: The N24, Non-Adiabatic Experiment". ECMWF Internal Report No.6.

Grimmer, M. & Shaw, D.B., 1967: "Energy preserving integrations of the primitive equations on the sphere". Quart. J.R. Met. Soc., 93, 337-349.

Gustaffson, B., Kreiss, H.O. & Sundstrom, A., 1972: "Difference approximations to mixed initial boundary value problems", II, Math. Comp., 26, 649-686.

Hollingsworth, A. & Geleyn, J-F., 1977: "A comparison of some diffusion operators in one and three dimensions". ECMWF internal working paper.

Holloway, J.L., Jr., & Manabe, S., 1971: "Simulation of climate by a global general circulation model: I Hydrologic cycle and heat balance". Mon. Wea. Rev., 99, 335-370.

Holloway, J.L., Jr., Spelman, H.J. & Manabe, S., 1973: "Latitude-longitude grid suitable for numerical time integration of a global atmospheric model". Mon. Wea. Rev., 107, 69-78.

Hoskins, B.J. & Simmons, A.J., 1975: "A multi-layer spectral model and the semi-implicit method". Quart. J.R. Met. Soc., 101, 637-655.

Janjic, Z. & Wiin-Nielsen, A., 1977: "On Geostrophic Adjustment and Numerical Procedures in a Rotating fluid". J. Atmos. Sci., 34, No. 2, 297-310.

Källberg, P., 1977: "Test of a lateral boundary relaxation scheme in a barotropic model". ECMWF internal report No. 3.

Kreiss, H.O., 1971: "Difference approximations for initial boundary value problems". Proc. Roy. Soc. Lond.A. 323, 255-261.

Kurihara, Y., 1965: "Numerical integration of the primitive equations on a spherical grid". Mon. Wea. Rev., 93, 399-415.

Kurihara, Y. & Holloway, J.L., Jr., 1967: "Numerical integration of a nine-level global primitive equations model formulation by the box method". Mon. Wea. Rev., 95, 509-530.

Lilly, D.K., 1964: "Numerical solutions for the shape-preserving two-dimensional thermal convection element". J. Atmos. Sci., 21, 83-98.

Mesinger. F., 1979: "Dependence of vorticity analogue and the Rossby wave speed on the choice of horizontal grid". Bulletin T. LXIV de l'Academie serbe des Sciences et des

arts, Classe des sciences mathematique et naturelles, Sciences Mathematique No.10, 5-15.

Mesinger, F. & Arakawa, A., 1976: "Numerical Methods used in Atmospheric models", Volume 1. GARP publications series No. 17.

Oliger, J. & Sundstrom, A., 1978: "Theoretical and practical aspects of some initial-boundary value problems in fluid dynamics". SIAM J. Appl. Math., 35, 3.

Richtmyer, R.D. & Morton, K.W., 1967: "Difference methods for initial value problems". Interscience Tracts in Pure and Applied mathematics No. 4. (2nd Edition), John Wiley & Sons.

Robert, A., Henderson J. & Turnbull, C., 1972: "An Implicit time Integration Scheme for Baroclinic models of the Atmosphere", Mon. Wea. Rev., 100, 5, 329-335.

Sadourny, R., 1975a: "The dynamics of finite difference models of the shallow-water equations". J. Atmos. Sci., 32, 680-689.

Sadourny, R., 1975b: "Compressible flows on a sphere". J. Atmos. Sci., 32, 2103-2110.

Simmons, A.J., 1979: "Angular momentum conservation in the ECMWF model". ECMWF internal memorandum.

Simmons, A.J., Hoskins, B.J. & Burridge, D.M., 1978: "Stability of the semi-implicit method of time integration". Mon. Wea. Rev., 106, No. 3, 405-412.

Sundstrom, A. & Elvius, T., 1979: "Numerical methods used in atmospheric models". Volume II, GARP publications series (to be published).

Tiedtke, M., Geleyn, J-F., Hollingsworth, A. & Louis,J-F., 1979: "ECMWF Model Parameterization of Sub-Grid Scale Processes". ECMWF Technical Report No. 10.

Temperton, C. & Williamson, D., 1978: "Normal mode Initialization for a multi-level Gridpoint model". ECMWF Technical Report No. 14.